Batch Emulsification Using an Inline Rotor-Stator in a Recycle Loop of Varying Volume

---

A dissertation submitted to the University of Manchester for the degree of M.Sc. in the Faculty of Engineering and Physical Sciences

2009

JONATHAN PAUL MANNING

SCHOOL OF CHEMICAL ENGINEERING AND ANALYTICAL SCIENCE

LIST OF CONTENTS

LIST OF FIGURES

LIST OF TABLES

Abstract

In industry emulsions are produced by recirculating the contents of a stirred tank through an inline mixer located in a recycle loop. The distribution of drop sizes in the stirred tank depends on the number of batch volumes, N_{BV}, that have been pumped around the loop. When scaling up pilot trials the value of N_{BV} is kept constant. One factor that changes between these scales is the size of the recycle loop relative to the size of the tank. The effect of this factor is unknown since existing models neglect the volume of the recycle loop.

This study extends an existing model of Baker (1993) to include the effect of a finite residence time in the recycle loop. Larger loop volumes are shown to lead to narrower distributions within the stirred tank and more rapid reduction of the fraction that has not passed through the mixer. On scaling up to industrial scales the recycle loop normally becomes proportionally smaller. Consequently if N_{BV} is held constant the results will not be as good as the trials: the distribution will be wider and less material will have passed through the mixer at least once.

An experimental study was conducted to investigate these predictions. At small recycle loop volumes the results from the literature were accurately reproduced. At larger recycle loop volumes it was possible to detect characteristic features of this extended model. However the shortcomings of the available inline mixer limited the contrast between the existing model and the proposed extension.

A rotor-stator was used as the inline mixer. A new method of representing the dispersive process as a matrix transformation has been developed. This allowed determination of the daughter droplet distributions without a priori assumptions of their form. These have been shown to be broader than the distributions normally assumed in the literature.

Declaration

I declare that no portion of the work referred to in the dissertation has been submitted in support of an application for another degree or qualification of this or any other university of other institute of learning.

Jonathan Manning

Copyright Statement

Acknowledgments

I am very grateful to my supervisor Dr. Peter Martin for his direction which focussed my experimental work and our discussions that developed my thinking.

Many thanks also to :

Adam Kowalski of Unilever for the generous loan of the Silverson mixer used in these experiments.

Craig Shore for skilfully fitting the equipment and his practical troubleshooting.

Dr. Mike Cooke for his help with matters practical and theoretical.

Liz Davenport and Eric Warburton for their patient help with the Mastersizer.

1. Introduction

Recycle loop volume: an unknown factor in the scale up of batch emulsification processes

The fine chemicals industry is characterised by a need for continual product development to maintain commercial advantages. This requires experimentation at laboratory and pilot plant scales. The results then need to be scaled up to industrial capacities. The process of scale up is fraught with difficulty and small errors at the trial stage can be magnified significantly. The annual cost of failed mixing scale up in the US alone is estimated to be $10 billion (Kresta et al 2004). In batch emulsification processes the finished product is made by recycling the contents of a stirred tank through an inline mixer. The resulting distribution inside the stirred tank is modelled in the literature (Baker 1993). Baker showed that at any time some of the material in the stirred tank will not have passed through the inline mixer whilst some will have passed through many times. This leads to wide drop size distribution. By calculating how much material has been through the mixer at any number of times Baker was able to predict how the drop size in the stirred tank evolved with time. Industrial processes are designed using the results of this model (Brocart et al 2002). However Baker's model neglects the volume of the recycle loop. The relative volume of the recycle loop compared to the batch volume is something that varies with scale. Because this has not been considered there is no understanding of how this impacts on the result of scale up. Small uncertainties at laboratory scale trials can cost millions of dollars at the industrial scale (Cohen 2005). Therefore it is very important that this effect be quantified. More reliable scale up will reduce the lead times for developing new products and reduce the risk of losses due to failure to produce the right quality of product.

The properties of emulsions and dispersions prepared in this way are dependent on the particle size distributions. For example clay filler can be added to asphalt to prepare a road surface layer (Cohen 2005). The value of this layer lies in its thixotropic rheology and this requires very thorough dispersion of the clay particles. Production of polymers via free radical polymerisation in colloidal dispersions is another example. In a polymerization reaction the ratio between Laplace pressure and osmotic pressure depends on drop size (El-Jaby et al 2007). A wide drop size distribution would lead to a wide range of reaction rates which would be undesirable. Clearly product design is related to controlling the drop size distribution. By understanding the impact of the recycle loop volume on the drop size distribution it will be possible to more accurately control the properties of these products.

The equipment used to make these products is not well understood. There is great secrecy around the performance of the rotor-stator mixers that are used to disperse the emulsions. The manufacturers maintain their competitive advantage by keeping a close guard on research data. There is not much publicly available information on their performance or how to scale up to larger mixers. There are many factors used to scale up rotor stator processes and the overall picture is confused. The voice of industry is clear that the procedure is, "more art than science," (Ryan and Thapar 2009), "often doesn't turn out as planned," (Shelley 2004) and is generally achieved through "trial and error," (D'Aquino 2004). The list of relevant factors is long and some are contradictory. Successful process design requires the selection of the most appropriate mixer for the job but this is not always straightforward: proprietary application guidelines for commercial mixers are a closely guarded secret (Cohen 2005); there is "almost no fundamental basis" to predict the performance of given design (Shelley 2004). Many experimental tests are "purely subjective" making definitive comparisons between different pieces of equipment very difficult (Ryan and Thepar 2008). These factors serve to hinder the development of new processes.

1.1. The scope of this work

A survey of the literature examines how the batch emulsification process has been modelled by neglecting the recycle loop volume. An experimental procedure for testing the model is critically assessed. This provides the background for modelling the effect of recycle loop volume and investigating the predictions. The issues relating to particular items of equipment are considered to aid the design of an experimental rig. The theoretical understanding of the dispersive process is examined. This allows consideration of the extent to which the existing methods can be applied to characterise rotor-stators.

The model in the literature is extended to include the effect of the recycle loop volume. To check its validity the solutions for a system with very small recycle loop volume are compared to the existing solutions from the literature. The characteristic effects of this new model are then identified. Example calculations show the significance of the findings for successful scale up and process development.

The experimental method outlined in the literature (Baker 1993) has been improved and applied to test the predictions of this new model. Comparison is made with the predictions of the existing model.

Finally a new concept of representing the effect of the inline mixer as a matrix transformation is investigated. This is shown to be an accurate model of the process. The

resulting matrix gives details of the daughter droplet distribution and breakage function that would not have been accessible through standard application of population balance models.

2. Literature Review

The primary aim of this work is to understand the effect of the recycle loop volume in batch emulsification systems. By reviewing how mixing field theory has been applied to analyse the process it is possible to see how to extend the existing model. The experimental system of Baker (1993) is the basis of the method followed here so it was important to review those techniques. When designing the experimental rig it is important to be able to relate the properties of the equipment to the assumptions in the model so some general issues around these items are investigated. In order to achieve the secondary aim of characterising the inline mixer it is important to understand how previous studies have tackled similar problems. This reveals the assumptions that are made and assesses whether they apply to rotor-stators or not. Finally, population balances have been used successfully to model dynamic dispersion processes. It is worthwhile to consider the strengths and weaknesses of this approach to the current problem.

2.1. Mixing field theory

The fine chemicals industry is driven by product innovation. A new formulation will have to meet certain specifications such as stability or sensory feel to be acceptable to the market. In practical terms these requirements may be expressed as constraints on average drop size or the drop size distribution (Brocart et al 2002). Experiments at the laboratory and pilot scales are necessary to determine how to achieve these goals. These results must then be scaled up to full size for a successful process. A recent review of mixing research explains how a proper understanding of the process requirements improves the chances of success at each stage . The old approach relied on design guidelines specific to each type of equipment and was inflexible with regard to developments in technology or non-standard mixing problems (Kresta et al 2004). The recommended alternative is to express process requirements in terms of mixing fields. A mixing field is characterized by the intensity of mixing and the residence time of a fluid element in the field. By similarly describing available equipment in terms of the mixing field produced it is possible to design the process by matching the requirements with the characteristics of appropriate mixers. Scaling up the equipment becomes a question of achieving the same mixing field at a larger scale. Kresta et al (2004) give the example of a stirred tank which can be modeled as containing two mixing zones: the impeller region where intensity is high but residence time low; and the bulk of the vessel where mixing intensity is of the order of 100 times lower but the residence time is longer. A crystallization process is cited as an example where this description is used with very good success. If the selectivity of a reaction is known to be controlled by micro-mixing then this determines the mixing

requirements: a mixing zone of high intensity. Such reactions are rapid so a short residence time in this zone is unlikely to be a problem. Comparison of the process requirements with the equipment properties shows that a stirred tank will satisfy the requirements if the reactant is fed directly to the impeller zone.

2.2. Batch Emulsification

A similar approach is used to analyse the process of manufacturing emulsions. The required mixing duty can be decoupled in to two parts: dispersive and distributive (Baker 1993). Distributive mixing refers to the blending requirement whereby the separate components of a mixture are to be distributed evenly throughout a product. Dispersive mixing is the breakup of the dispersed phase droplets to smaller sizes. This might be to increase the rate of mass transfer between the phases or to stabilize the emulsion if it is the end product. Stirred vessels are readily available in the fine chemicals industry due to their versatility. They can supply a mixing field capable of meeting the distributive needs but cannot reach the intensity required for a high degree of dispersion. Baker (1993) recommends incorporating an external in-line mixer in to a recirculation loop so that the distributive and dispersive zones can be designed separately. This arrangement is shown in Figure 2.1.

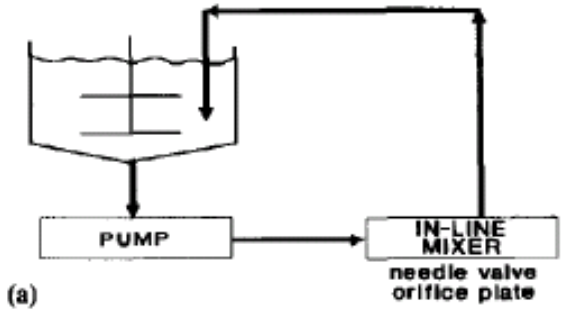

Figure 2.1 Showing the equipment for Batch Recirculation Emulsification (Taken from Baker 1993)

Brocart et al (2002) point out that this leads to a wide range of droplet size. The cause of this is that during operation some of the tank's content will not have passed through the recycle loop whereas some will have passed through many times. Brocart et al were looking at a water-in-diesel emulsion as a cleaner fuel for which stability is crucial. A narrow distribution of water droplet sizes was found to be more stable than a poly-disperse product.

2.2.1. Theoretical modelling

Clearly then it is a matter of practical importance to determine the fraction which has not passed through the loop and that which has passed through any given number of times. Baker (1993) shows how this can be done by using a model with two assumptions: the stirred tank is well mixed and the volume of the recycle loop is negligible. The initial condition is that at time t=0 then C_0=1 where C_0 is the volume fraction in the tank that has not passed through the inline mixer. The assumption of a well mixed tank leads to a mass balance on C_0 of

Equation 2.1

$$\frac{dC_0}{dt} = -\frac{F}{V}C_0$$

Where F is the flowrate round the recycle loop and V is the volume of the tank. The solution is

Equation 2.2

$$C_0 = e^{\frac{-Ft}{V}} = e^{-N_{BV}}$$

Where $N_{BV} = \frac{Ft}{V}$ is the number of batch volumes that have been pumped round the recycle loop. In general C_i is the volume fraction in the tank that has passed through the inline mixer i times and the relevant mass balance is (Baker 1993),

Equation 2.3

$$\frac{dC_i}{dt} = \frac{F}{V}\left(C_i^{'} - C_i\right)$$

$C_i^{'}$ is the volume fraction of the material returning to the tank that has passed through the inline mixer i times. By neglecting the recycle loop volume the material is assumed to take no time to pass through the loop which leads to the identification,

Equation 2.4

$$C_i^{'} = C_{i-1}$$

Using this relationship to solve Equation 2.3 Baker (1993) found the general solution to be,

Equation 2.5

$$C_i = \frac{e^{-N_{BV}} N_{BV}^{\,i}}{i!}$$

Baker is comparing volume fractions so the relevant average is the volume weighted mean. For a discrete distribution where d_j is the mid-point diameter of the j^{th} size class and θ_j is the volume fraction in that size class then the volume weighted mean diameter is given by,

Equation 2.6

$$d_{43} = \sum_j \theta_j d_j = \frac{\sum_j n_j d_j^4}{\sum_j n_j d_j^3}$$

n_j is the number of particles in the j^{th} size class. If $d_{43}(i)$ is the volume weighted mean diameter after i passes through the inline mixer then the mean diameter of the mixture is given by,

Equation 2.7

$$d_{43} = \sum_{i=0}^{\infty} C_i d_{43}(i) = \sum_{i=0}^{\infty} \frac{e^{-N_{BV}} N_{BV}^{i}}{i!} d_{43}(i)$$

Since $d_{43}(i)$ is shown to be independent of flowrate then d_{43} is only a function of N_{BV}. That is why N_{BV} is used as a variable in scaling up these processes. Baker compared this expression with measured values taken over a period of an hour while the recycle loop was operating and the agreement is described as excellent.

2.2.2. Experimental investigation

These predictions are confirmed by a series of experiments described in the same paper. Two types of inline mixer are used: an orifice plate and a needle valve. Initial experiments characterise the mixers in terms of the average drop size after i passes through the mixer. To find this information the whole batch is passed through the inline mixer in a single pass in to a separate container. A sample is taken and the process is repeated. 5 passes are reported for the orifice plate and 10 for the needle valve but in neither case is a stable limit reached. For both devices the greatest reduction occurs in the first pass and the rate of drop size reduction declines for subsequent passes. This gives the values of $d_{43}(i)$ which are used with Equation 2.7 and Equation 2.5 to predict the average drop size in the stirred

tank. After this data has been found pilot scale batch emulsifications are performed. The recycle loop returns the processed emulsion to the stirred tank and the drop size is measured at different times. The predictions of Baker's model provide a good fit to the measured data and confirm the theoretical model.

Baker is able to further validate his model by looking at the evolution of the drop size distribution. The distributions after *i* passes can be combined, weighted with the values of C_i, to predict the distribution after a given time. The results are very clear and support his conclusion. This is helped because his inline mixers produce an order of magnitude change in drop size. In systems where less drastic changes are produced then the evolution of the drop size distribution might be less easy to discern with the naked eye.

A similar experimental investigation is necessary for the present work so it is important to recognize some problems with Baker's method. To create an initial emulsion in the stirred tank Baker pours the oil phase on to the surface of the aqueous phase. This is not an efficient way of mixing the phases (El-Hamouz et al 2009) as it can lead to large droplets staying on the surface and not being entrained in to the bulk. More seriously he defines $t = 0$ at the moment the oil is poured on to the surface. There are many studies showing that in a stirred tank the equilibrium drop size is not reached until a period of the order of 1 hour (Pacek et al 1998, Calabrese et al 1986a, Arai et al 1977). Application of Equation 2.7 implicitly assumes that $d_{43}(0)$ is constant i.e. that there is no drop breakup in the tank. This will not be true in Baker's experiment. The reason that his results are not compromised is that his inline mixer achieves almost an order of magnitude reduction in drop size. The effect of the inline mixer outweighs the marginal decline in $d_{43}(0)$ with time. An additional consequence of both these problems is the variation in $d_{43}(0)$ between batches. (NB- Baker prepares a master batch of each phase to ensure consistency but for each experiment a new batch of emulsion is created in the tank and this is the batch referred to here.) This in itself might not be a problem but it is not clear that Baker is consistent in addressing it. In Baker (1993) the values of $d_{43}(i)$ are reported for both the orifice plate and the needle valve. The $d_{43}(0)$ value for the orifice plate is ~50 μm and for the needle valve it is less than 40 μm. This is not consistent with his comparison between the predictions of Equation 2.7 and his experimental results. In this case he uses $d_{43}(0)$ =50 μm for both cases. The fit looks like it would be improved if the value of 40 μm were to be used for the needle valve. Because of this it seems likely that 40 μm would be the correct value and that Baker has made an oversight. Again the effect is small in

comparison to the large change due to the inline mixer so it does not affect his conclusion. In future work attention should be paid to this point.

2.2.3. The need to include the recycle loop volume

The setup shown in Figure 2.1 represents the simplest case. In industrial applications it is sometimes necessary to incorporate an additional loop around the inline mixer (Brocart et al 2002). This effectively increases the residence time in the high shear mixing field. If the residence time is increased significantly then the assumption of a negligible residence time will become invalid.

2.3. Experimental considerations

In order to commission an experimental rig to perform a similar investigation it is necessary to consider the properties of the available equipment. Batch emulsification requires a stirred tank, an inline mixer, a pump and pipework connecting it all together. In addition the physical properties of the emulsion need to be considered when designing the experiments.

2.3.1. Physical properties of emulsions

The principle properties of interest for this experiment are the viscosity and resistance to coalescence. These need to be known in order to calculate the flow regime in the pipes and ensure that the emulsion is stable to match the assumptions of the theoretical model.

The viscosity of an emulsion is given by,

$$\mu = \mu_c(1 + 2.5\phi)$$

Where μ_c is the continuous phase viscosity and ϕ is the dispersed phase volume fraction. This has been successfully applied at phase fractions up to 10% so will cover the range used in this work (Becher 2001).

The presence of surfactant reduces the interfacial tension and stabilises the emulsion. To ensure the greatest reduction in interfacial tension it is necessary to use a surfactant concentration above the critical micelle concentration (cmc). To eliminate the effect of dynamic surface tension it is necessary to operate significantly above the cmc (Koshy et al 1988). As the oil droplets are dispersed the interfacial area increases. More surfactant will adsorb at the interface and deplete the concentration in the bulk. This effect needs to be accounted for. The surfactant used, SLES, has a cmc of 0.2 mmol l^{-1} and an average molecular weight of 420 (El-Hamouz 2007). The head group for a range of surfactants was found to occupy 0.6 nm^2 at the interface (Goloub et al 2003). SLES was not one of

these surfactants but this will serve as a useful estimate. Using these values it is possible to calculate the concentration of surfactant in the bulk. If the aqueous phase is 1% SLES by weight, the dispersed phase fraction is 5 % by volume and the drop diameter is 1μm then the concentration in the bulk will still be more than 100 times the cmc.

The surfactant ensures that the emulsion is stable against coalescence. The continuous phase is not very viscous so the emulsion will be prone to creaming. This will not cause any problems because the agitation in the stirred tank will be enough to keep the emulsion well mixed.

2.3.2. Tall tanks

For agitated tanks of standard geometry the blending process is well documented in standard textbooks. For a non-standard geometry, such as a tall tank it is necessary to confirm whether and under what conditions standard results apply. Then the equipment can be evaluated to see if it matches the requirements.

The mixing regime is turbulent for tank Reynolds numbers of order 10^4 or more. For geometrically similar tanks the product Nt_{95} is a constant (Miller 2009). Numerical models incorporating turbulent mixing and flow patterns can be used to estimate t_{95}. The tall tanks are modelled as consisting of several ideally mixed cells with intracellular flow between adjoining cells. This is justified because the agitators are hydro-dynamically distinct provided that they are sufficiently separated. The minimum separation is interpreted differently by different studies: either twice the impeller diameter (Jahoda and Machon 1994) or the tank diameter (Alves et al 1997). These are both the same order of magnitude so there is a clear rule of thumb to estimate if this effect needs to be taken in to account.

Jahoda and Machon (1994) found that for 2, 3 and 4 impellers the dimensionless mixing times Nt_{95} were respectively ~80, 200 and 400. By comparison the study by Alves et al (1997) found values of ~ 100 and 200 for 2 and 3 impellers respectively. In both cases the results were independent of Reynolds number. Clearly the mixing time increases with the number of stages due to the limited mass transfer between cells.

This effect may sometimes be desired and horizontal donut baffles can be added to reduce mass transfer between the zones. If the flow in and out of the tank is at opposite ends then 4 to 6 of these zones create a very good approximation to plug flow (Hemrajani 2004). This combination of mixing and plug flow has applications in many processes such as extraction, dissolution and polymerization.

The effect of impeller geometry is not clear. Ranada et al (1991) claim that a downflow pitched blade turbine is most efficient for liquid phase mixing. Jahoda and Machon (1994) found that pitched blades are more efficient than Rushton turbines but that the direction of impeller pumping did not affect the mixing time. From an experimental point of view the most important thing is consistency so if pitched blades are used the direction of pumping should be held constant.

In the context of a recirculating batch emulsification loop the main vessel will be considered well mixed if the mixing time is short compared to the characteristic residence time V/F. The results above allow an order of magnitude estimate of the dimensionless mixing time to be made for comparison. If there is large density difference between the two phases of an emulsion the mixing times will be greater than these predictions.

2.3.3. Pipework

Mixing occurs not only in the dedicated devices but also in the pipes as the fluid flows through them. In order to incorporate the recycle loop volume in to Baker's model it is necessary to understand the mixing field in the pipe. Dispersive mixing is best considered in the context of the general theory of dispersive mixing. In this section the distributive mixing field will be examined and this depends on the flow regime.

Turbulent flow is the simplest case. Turbulent flow in pipes is generally modeled as plug flow. Perfect radial mixing and a single residence time for all fluid elements are assumed. The random eddies are responsible for the radial mixing and an empirical rule of thumb states that this occurs over a pipe length approximately 100 times the pipe's diameter (Etchells and Meyer 2004). Since the eddies occur in all directions they also cause axial mixing and it seems reasonable that axial mixing will occur at a similar rate to radial mixing. This gives a very crude estimate that the length of axial mixing is 1/100th of the pipe length. In terms of the residence time this is a variation of 1% so plug flow is a reasonable assumption. However random walk processes proceed with the square root of time so whilst this might be a useful first estimate it does not give a good understanding of the phenomena. Soluble salts in turbulent water pipes diffuse with a virtual coefficient of diffusion *k* given by (Taylor 1954),

$$D_{turbulent} = 10.1 a v^*$$

Where *a* is the pipe's internal diameter and $v^* = \sqrt{\tau_W / \rho}$ is the wall friction velocity. Taylor develops this approach to model how the interface between two elements of fluid

develops with time. The characteristic length of the axial mixing, *S*, in a pipe of length, *L*, is given by (Taylor 1954)

Equation 2.8

$$S^2 = 437aL\frac{v^*}{u}$$

u is the mean velocity in the pipe. The formula matched experiments where two different types of gasoline were pumped along the same pipe, one after the other.

This shows that it is reasonable to model the turbulent flow in a pipe as plug flow and that the degree of deviation from this ideal can be readily estimated.

In laminar flow there is a strong variation in velocity over the cross section and fluid elements follow the streamlines. This leads to a wide variation in residence times. For the diffusion of soluble salts in laminar flow there are two regimes. If the molecular diffusion is slow then the variation in residence times is determined by the radial velocity variations. If molecular diffusion is fast then it leads to radial mixing in addition to the axial mixing. Diffusion becomes important when (Taylor 1953a),

Equation 2.9

$$\frac{L}{u_0} >> \frac{a^2}{3.8^2 D_{mol}}$$

Where u_0 is the peak velocity in the pipe and D_{mol} is the molecular coefficient of diffusion. In an emulsion the diffusion would be due to Brownian motion of the droplets. For this process the coefficient of diffusion is (Becher 2001 p.74),

Equation 2.10

$$D_{Brownian} = \frac{k_B T_{Kelvin}}{3\pi\mu_c d}$$

k_B is the Boltzmann constant, T_{Kelvin} the absolute temperature in degrees Kelvin, μ_c is the viscosity of the continuous phase and *d* is the droplet diameter. For droplets ~50 μm across at room temperature suspended in water then,

$$D_{Brownian} = \frac{1.38\times10^{-23}\times298}{3\pi\times10^{-3}\times50\times10^{-6}} = 8.7\times10^{-15}$$

So for a pipe of radius 5mm diffusion will only become significant when the residence time is greater than,

Equation 2.11

$$\frac{\left(3\times10^{-3}\right)^2}{3.8^2\times8.7\times10^{-15}}=2\times10^8\,\mathrm{s}$$

The time constraints of a three month dissertation rule out an investigation of this regime so diffusion in the pipes will be ignored.

The radial variation in velocity in laminar flow is then given by (Taylor 1953a),

Equation 2.12

$$u(r)=u_0\left(1-r^2/a^2\right)$$

This can be used to determine the residence time distribution if necessary.

The literature shows that plug flow is a reasonable model for turbulent flow in pipes. The degree of axial mixing can be estimated to check whether it could affect the modelling. In laminar flow the residence time distribution will need to be taken into account. This information can be used to understand the effect of the recycle loop volume in batch recirculation emulsification.

2.3.4. Rotor Stators

Rotor-stators are used in industrial applications where high shear mixing is required. Compared to conventional mechanical agitators they are not well understood. There has been little fundamental research into them and commercial incentives mean that what work is done is often not widely available. A review of some available scientific work and the trade press reveals the current level of knowledge and suggests which areas would benefit from further investigation.

The defining feature of a rotor-stator is a high speed rotor in close proximity to a stator. The gap between rotor and stator is typically 100-3000 μm and rotor tip speeds are of the order 10-50 m s^{-1} (Utomo et al 2009). The maximum shear stress is achieved in this gap (Barailler et al 2006) and reaches values of 100,000 m s^{-1} (D'Aquino 2004). The stator surrounds the rotor and is perforated with narrow openings, the exact size and shape of which vary between designs. The agitated liquid flows through these holes as jets (Shelley

2004). The velocity of the jets is proportional to the rotor tip speed (Utomo et al 2009). Computational fluid dynamics has been used to show that it is not the mechanical forces in the shear gap that are responsible for dispersion (Barailler et al 2006). Rather dispersion occurs in the jets discharged from the slots. The resulting flows are assumed to be highly turbulent (Bourne and Studer 1992) and capable of providing high intensity mixing for a variety of applications.

In assessing the level of turbulence in the rotor stator Barailler (2006) has pointed out that the Reynolds number is ambiguous. By analogy with stirred tanks it could be defined,

$$\mathrm{Re} = \frac{\rho\, ND^2}{\mu}$$

But in the high shear region it could be defined,

$$\mathrm{Re} = \frac{\rho\, ND\delta_{gap}}{\mu}$$

Where δ_{gap} is the width of the gap between rotor and stator. In addition when you consider that turbulence in the jet region is responsible for dispersive mixing then a third variation presents itself,

$$\mathrm{Re} = \frac{\rho\, NDb}{\mu}$$

Where *b* is the width of the hole in the stator. This might seem like splitting hairs but there is at least an order of magnitude difference between each one.

Whilst the level of turbulence indicates the strength of the mixing field it is not very useful for predicting performance. Specific power has been successfully used to correlate mixer performance across a wide range of technologies (Davies 1987). The overall power consumption in rotor stators is controlled by a power number as for standard agitators so,

Equation 2.13

$$P = P_0 N^3 D^5 \rho$$

The rotation causes the mixer to act as a centrifugal pump. Typical of such pumps the Power number is proportional to the flowrate (Utomo et al 2009). Typical values of the power number are 3 (Barailler et al 2006) for a head made by VMI Rayneri (France) and 1.7-2.3 (Utomo et al 2009) for a Silverson L4RT, depending on the stator. The choice of

stator also affects the particle size distribution (Ryan and Thapar 2008). One possible reason for this is that narrower slits have a more even distribution of ε across them and this would cause a narrower drop size distribution. Brocart (2002) shows that the energy dissipation rate in the stator hole is given by,

Equation 2.14

$$\varepsilon \approx \frac{\rho (ND)^3}{4b}$$

This is an interesting result since is predicts that the rotor stator's performance should be equally well correlated by tip speed or local energy dissipation rate.

Even if ε can be successfully used to correlate a rotor-stator's performance it gives no information about the breakage kinetics. There is a great need for an "underlying mathematical representation to model and predict," the operation of these mixers (Shelley 2004). The field of population balances has been applied to this end to investigate agitated tanks and offers the opportunity to explain rotor-stators (Kowalski 2008). So in order to better characterise rotor stators it is important to understand the work that has already been done towards characterising stirred tanks.

2.4. General theory of droplet dispersion

The break-up of droplets in high Reynolds number flows is caused by dynamic forces in the continuous phase. These forces are resisted by the viscosity and surface tension of the dispersed phase droplets. This process is most often explained in the literature in terms of early work on the structure of turbulent flows and the deformation of drops that is collectively known as the Kolmogorov-Hinze theory of droplet breakup.

2.4.1. Kolmogorov turbulence

The fluid velocity at any point in turbulent flow may be thought of as having an average value upon which is superimposed a random vector (Kolmogorov, 1941a). These random eddies exist on a range of scales from the macroscopic scale of the equipment down. Kolmogorov states that these macroscopic eddies absorb energy from the fluid motion and pass it on in turn to smaller scale eddies. This energy transfer is achieved through a process called vortex stretching (Baldyga and Bourne, 1999, p62). Velocity fluctuations in one direction create smaller velocity fluctuations in other directions and energy cascades down the length scales. At sufficiently small scales the viscosity becomes important and the motion is dissipated to the internal energy of the fluid. The characteristic length, η, of these smallest eddies is given by (Kolmogorov 1941c),

Equation 2.15

$$\eta = \frac{\nu^{3/4}}{\varepsilon^{1/4}}$$

Where ν is the kinematic viscosity and ε is the rate of energy dissipation per unit mass.

The large number of intervening steps in the energy cascade randomizes the velocities of the fluctuations at sufficiently small scale. For scales much smaller than the largest eddies the fluctuations can be considered as isotropic (Kolmogorov 1941a). This means that the velocity fluctuations have no preferred direction and their probability distribution function (PDF) is steady with respect to time.

To calculate the dispersive effects of this isotropic turbulence more detail is needed about the probability associated with fluctuations on a particular scale and with a particular velocity. Kolmogorov (1941a) introduces two hypotheses of similarity that can be used to theoretically determine these probabilities. Firstly the distributions in isotropic turbulence are uniquely determined by the kinematic viscosity, ν, and the energy dissipation rate, ε. Secondly if the scale of the eddies is also large with respect to the Kolmogorov length scale, η, then the PDF is a function solely of the energy dissipation rate, ε. The range of length scales, $D >> d >> \eta$, over which the second hypothesis applies is known as the inertial subrange.

The energy spectrum of the turbulence can be found by applying dimensional analysis in conjunction with the second hypothesis. For an eddy of length l the wavenumber is defined $k = 1/l$ and the energy spectrum is given by (Frisch 1995, p92),

Equation 2.16

$$E(k) = \alpha \varepsilon^{2/3} k^{-5/3}$$

where α is a dimensionless constant. In the inertial subrange a similar analysis is used to find the mean square relative velocity of two points separated by a distance l (Baldyga and Bourne 1999, p83),

Equation 2.17

$$\left\langle \left(u(l)\right)^2 \right\rangle = (\varepsilon\, l)^{2/3}$$

This last result is known as the two-thirds law.

Kolmogorov's assertions are not proved in his papers but there have been later experimental studies to show that the results are valid: the turbulent energy spectrum of helium flow between two rotating cylinders has been shown to follow the $k^{-5/3}$ dependence over several orders of magnitude (Maurer, J. et al 1994); and experiments in wind tunnels (Frisch 1995, p 58) have empirically verified the two-thirds law.

The inertial subrange in a rotor stator can be estimated. Dispersion occurs in the jets flowing out of the stator holes so the relevant macroscopic length is the width of the stator holes, not the diameter of the rotor. Typically this is around 1 mm. The rotor diameter of a Silverson L4RT is 28.2 mm and 5000 rpm is a realistic operating speed (Utomo et al 2009). Using Equation 2.14 to calculate the energy dissipation rate in the jet and substituting in to Equation 2.15 the Kolmogorov length is approximately 0.2 μm for water. The largest drops being dispersed are approximately 0.5 mm in diameter and the smallest daughter drops are about 1 μm across. So the drop sizes of interest do not fall well within the boundary of the inertial subrange. Therefore it is not clear that isotropic turbulence can be assumed as the cause of droplet breakup in rotor-stators. It is worth assessing how crucial the assumption of isotropic turbulence really is for understanding dispersion in stirred tanks. This will show to what extent the existing analysis can be applied to rotor-stators.

2.4.2. Hinze theory of inviscid droplet stability

The dispersive process can be understood by considering the forces acting on an individual droplet of diameter *d*. An external force per unit area of τ disrupts the surface of the drop and the surface tension, σ, resists. The magnitude of the restoring force per unit area is σ/d. The ratio between the external stress and the stabilizing force of surface tension is known as the generalized Weber number,

Equation 2.18

$$We = \frac{\tau\, d}{\sigma}$$

The fundamental principle of drop breakup is that if the Weber number exceeds a critical value, We_{Crit}, then the particle will be dispersed (Hinze 1955). However the critical value is not constant but depends on the system. Taylor (1934) showed experimentally that the

critical value depended on the type of flow and on the ratio between the viscosities of the continuous and dispersed phases.

Hinze assumes that the external force is due to the dynamic pressure of eddies of the same size as the drop. Assuming isotropic turbulence he uses Equation 2.17 to find the velocity of these eddies giving,

Equation 2.19

$$\tau = \frac{\rho_c (\varepsilon d)^{2/3} d}{\sigma}$$

Equation 2.19 in combination with Equation 2.18 show that the Weber number increases with drop size. Consequently there will be some maximum drop size, above which $N_{We} > N_{We,crit}$, and drops larger than this will be unstable. Equation 2.18 and Equation 2.19 can be combined to give,

Equation 2.20

$$\frac{\rho_c \varepsilon^{2/3} d_{\max}^{5/3}}{\sigma} = Z_2$$

Where Z_2 is a constant particular to the system. A review of several studies (Shinnar and Church 1960) has confirmed this result.

Hinze recognizes that the turbulence in a stirred tank is not isotropic since the intensity is greatest nearest the paddles. To apply the foregoing analysis he states that, "it must be assumed that turbulence pattern is practically isotropic in the region of wavelengths comparable to the size of the largest drops." The contention that at least local isotropy must be assumed is not necessarily true. Equation 2.20 can be derived from dimensional analysis. Therefore it does not depend on the precise mechanical form of droplet breakup. Equation 2.20 is consistent with the outlined model of isotropic turbulence but does not depend on it. In any system where the drop size is determined only by ε, ρ_c and σ then Equation 2.20 will apply regardless of the nature of the destabilizing forces. This is important because much of the literature is concerned with experimentally verifying this relationship and then implying that drop breakup in a given system is caused by isotropic turbulence. The erroneous subtext throughout is that this relationship will not apply where isotropic turbulence is absent.

2.4.3. Observations of droplet breakup in non-isotropic turbulence

Turbulent drop breakup had been observed in stirred tanks (Ali et al 1981, Chang et al 1981). It was only observed in very turbulent flow where $\mathrm{Re} > 10^7$. For pitched blade turbines dispersion only occurred in the immediate region of the blades. For disc style turbines turbulent break-up was also observed in the vortex system that extends radially from the agitator. Photographic recordings showed that on entering the vortex region the drops, "simply disintegrated into a cloud of smaller drops," (Chang et al 1981). However for intermediate Reynolds numbers ($10^4 < \mathrm{Re} < 10^7$) the same researchers described a different drop breakup mechanism: ligament stretching. A particle near the turbine is stretched in to a ligament or sheet in the vortex region. At a certain point it is stretched so thin that surface tension causes it to break up in to many smaller droplets. This mechanism is not consistent with the sudden impact of a random turbulent eddy.

Whilst looking at transient drop size distributions Konno et al (1983) captured photographic evidence of the spatial distribution of drop breakup in a stirred tank. This clearly showed two separate regions; one identified as isotropic turbulence because the direction of deformation was random; the second as non-isotropic because the axis of deformation was always aligned with the direction of flow rotation.

Observations of dispersion in pipes showed that droplets only broke up near the wall and not in the main flow (Sleicher 1962). The turbulence near the wall is dominated by eddies of macroscopic scale which are not isotropic (Baldyga and Bourne 1999). Another study showed that velocity of dispersive eddies was proportional to agitator tip speed (Davies 1987) which would not be the case for isotropic turbulence.

These observation shows that it is possible to objectively confirm that in some flow regimes isotropic turbulence is not the cause of droplet breakup. In all these situations isotropic turbulence is commonly cited as the mechanism but clearly this has no basis. Consequently the correlations developed should apply just as well to rotor-stators even if the turbulence is not isotropic.

2.4.4. Correlating droplet size in stirred tanks

The majority of work on dispersing emulsions has been conducted in stirred tanks. Understanding how stirred tanks have been characterised sheds light on the issue of how to characterise rotor-stators. For stirred tanks the relationship of Equation 2.20 is usually expressed in a different way. The energy density is given by, (Calabrese et al 1986)

Equation 2.21

$$\varepsilon \propto N^3 D^2$$

where N is the rotational speed in r.p.m and D is the agitator diameter. The tank Weber number is defined

Equation 2.22

$$We = \frac{\rho_c N^2 D^3}{\sigma}$$

Substituting these in to Equation 2.20 gives,

Equation 2.23

$$\frac{d_{\max}}{D} \propto We^{-3/5}$$

Which is the well known Weber correlation. In most investigations only the rotational speed is varied since the geometry of the tank and the physical properties of the fluid are constant. In this case the observed relationship is,

Equation 2.24

$$d_{\max} \propto N^{-1.2}$$

The overall power consumption of a rotor stator is given by

Equation 2.21 but the relevant rate of energy dissipation is not the average rate but the rate in the dispersion zone of the jets. The local energy dissipation here is given by Equation 2.7 instead. This has the same dependence on N but not D. This means that for a given rotor-stator Equation 2.24 shouldhold. Upon scale up however D will change and so

Equation 2.23 will not be valid. These correlations apply in the inviscid limit where the drop size is determined only by ε, ρ_c and σ. In many industrial situations the dispersed phase is viscous, or present at high phase volume or stabilised by surfactant. Therefore it is important to consider these affects also.

2.4.5. The effect of surfactant

For the production of many commercial emulsions a surfactant will be used to stabilize the mixture. This reduces the interfacial tension and from Equation 2.20 we can predict that this will lead to smaller droplets. However it has been shown (Koshy et al 1988) that

accounting for the reduction in surface tension in this manner will significantly overpredict the observed maximum drop size. The effect is attributed to dynamic surface tension. When a spherical drop is deformed its surface area increases. If the deformation occurs in a timescale shorter than the timescale for the adsorption of surfactant at the interface then the local area concentration of surfactant will decrease. This will cause a local increase in interfacial tension. This increased value is called the dynamic interfacial tension, $\sigma_{dynamic}$. Koshy et al (1988) argue that the difference in interfacial tension (higher near the deformation, lower elsewhere) causes flows inside the droplet which exacerbate the deformation and aid the dispersion of the particle. By incorporating an extra deforming stress, $\frac{\sigma_{dynamic} - \sigma}{d}$, in to Hinze's model they calculated the effect on drop size. They compared a surfactant free water-octanol system with a water-styrene-surfactant system that had the same interfacial tension. They correctly predicted the difference between the two sets of data. They showed that $\sigma_{dynamic} - \sigma$ was a function of surfactant concentration. Unlike many other properties this did not show an abrupt change at the critical micelle concentration (cmc). The difference increased from zero at very low concentration to a peak and then fell to zero at high concentrations. For the largest value of $\sigma_{dynamic} - \sigma$ the effect was a decrease in the drop size by a factor of ½. The immediate practical consequence of this is that surfactant concentration should be held constant in order to produce a consistent drop size.

2.4.6. The effect of dispersed phase fraction

In industrially relevant emulsions the dispersed phase often occupies a significant volume fraction. Desnoyer et al (2003) investigated the effect that this had on the Sauter mean diameter. For a system showing minimal coalescence they found that,

Equation 2.25

$$\frac{d_{32}}{D} = 0.14(1 + 0.48\phi)We^{-3/5}$$

Where ϕ is the dispersed phase fraction. This is physically interpreted as representing the dampening of the turbulence due to the dispersed phase absorbing the turbulent eddies. The review of the literature (Calabrese et al 1986b) also affirms the form of this relationship for high phase volumes. Although they caution that there is a lack of experimental work regarding high phase fractions of viscous droplets.

The drop size is more sensitive to phase fraction when there is coalescence. An iso-octane and carbon tetrachloride in water dispersion is explored at phase fractions up to 34 % (Mlynek and Resnick 1972). Under these conditions it was found that the mean drop size was well correlated by

Equation 2.26

$$\frac{d_{32}}{D} = 0.058(1 + 5.4\phi)We^{-3/5}$$

For an emulsion stabilised by surfactant there won't be coalescence so the influence of phase fraction will be small. Nevertheless this shows that in the experimental design the dispersed phase fraction will need to be controlled.

2.4.7. The effect of dispersed phase viscosity

Many commercial products involve viscous dispersed phases so it will be important to characterise how the performance of rotor-stators is affected by this variable. The results show that the physical properties of the emulsion are more important than the nature of the turbulence in determining the drop size distribution. In addition it seems that the degree of dependence on dispersed phase viscosity can reveal a lot of information about the breakage mechanism.

Dimensional analysis (Hinze, 1955) shows that the process can be described by two independent dimensionless groups. Taking the Weber number as the first group the second is the viscosity group given by,

Equation 2.27

$$N_{Vi} = \frac{\mu_d}{\sqrt{\rho_d \sigma\, d}}$$

N_{Vi} is a measure of the relative importance between viscosity and surface tension in stabilising the particle. Larger values of the viscosity group imply a larger effect due to the viscosity.

By considering the harmonic oscillation of a drop Sleicher (1962) shows that the viscous resistance to deformation is well represented by Hinze's viscosity group. However it is pointed out that this result is only valid for small deformations. Therefore the breaking of a drop is expected to deviate from this regime. By considering the viscous flows in a stretching drop an alternative viscosity group is suggested,

$$Vi = \frac{\mu_d \, \bar{u}_c}{\sigma}$$

Where $\bar{u}_c$ is the mean velocity of the continuous phase. This is a useful development and has been adopted by later researchers (Calabrese et al 1986a) who incorporated a factor for the relative densities,

Equation 2.28

$$Vi' = \sqrt{\frac{\rho_c}{\rho_d}} \frac{\mu \, \bar{u}_c}{\sigma}$$

The stability of viscous drops was studied by Arai et al (1977). The resistance to deformation was modeled as a Voigt element. This is a spring and dashpot connected in parallel. This model independently finds that the viscosity group *Vi'* as used by Calabrese et al (1986) is the correct one.

The viscous contribution to the stabilising energy barrier is of the order (Calabrese et al 1986a),

Equation 2.29

$$\mu_d d^2 \sqrt{\frac{\tau}{\rho_d}}$$

This leads to a modified expression for the Sauter mean diameter,

Equation 2.30

$$\frac{d_{32}}{D} \propto \left(1 + BN_{Vi}\right)^{3/5} We^{-3/5}$$

This model was experimentally tested but Calabrese was unable to fully explain the results. For viscosities of 0.1 – 0.5 Pa s the correlation worked and *B* was found to be equal to 11.5. For an intermediate viscosity of 1 Pa s the formula did not fit the experimental data. However as μ_d is increased further to 5 and 10 Pa s the model can be fitted but requires a smaller value of *B*. Calabrese expected *B* to increase with increasing viscosity. By considering how the breakage mechanism changes the observed result can be explained. The Sauter mean depends on the droplet distribution which is characteristic of the breakage mechanism and not of the turbulent spectrum as claimed by Chen and Middleman (1967). It has been shown that in viscous flows (Hinze 1955, Taylor 1953) that the maximum drop

size depends on the nature of the flows. This shows that different patterns of deformation induce different levels of resistance from the surface forces. Two ideas follow from this. Firstly a deformation involving large internal flows will be stabilized more by viscosity than one that does not. Secondly the mode of breakage observed will be that with the lowest overall resistance. Consider two modes of breakage: one which involves a minimum of surface deformation and large internal flows; the second has smaller flows but larger surface deformation. In the inviscid limit the first will be preferred since surface tension is the only resistance. As the viscosity is increased the stability against deformation of the first type will increase most rapidly since it involves the largest velocity gradients. At some point the two types will be equally stable and further increases in viscosity will result in the second mechanism becoming preferred. The crucial point is that this second mechanism is less sensitive to viscosity as it involves smaller internal shear rates. In the context of Equation 2.30 this means a smaller value of B. This explains the observed result that B decreases as viscosity increases. It also predicts that if higher values of viscosity were tested then B should only decrease further. Speculating on deformations that minimize internal flows one imagines ripples at the surface that do not penetrated deeply in to the body of the drop so as to minimize the amount of fluid displaced. These ripples would produce daughter droplets much smaller than the parent. Calabrese (1986a) noticed a larger number of small drops as the viscosity increased. Other workers have also suggested that breakup of viscous drops consists of pinching of small drops and this suggests an explanation for why it should be so.

Further work is reported (Wang and Calabrese 1986) which investigates the relative influence of viscosity and interfacial tension. Over the range of viscosity from $10^{-3} - 1$ Pa s all the data was well correlated by Equation 2.30. This implies a consistent mode of droplet breakup. The changes in viscosity and surface tension cover four and two orders of magnitude respectively. The constancy of the breakage mode suggests that there are not very many possible breakage modes.

Davies (1987) uses the same viscosity group as Sleicher (1962) and Calabrese et al (1986a) to analyse breakage in valve and sonic homogenisers. He found that this was the correct correlating factor but that the relative effect of μ_d varied between systems. Where breakup was relatively slow (in stirred tanks) he argues that there is significant deformation before breakage so the elongational viscosity will cause resistance. For Newtonian fluids the Trouton ration relates the shear and elongational viscosity, $\mu_{elongational} = 3\mu_{shear}$. In the homogenisers the breakup is more rapid and there is assumed to be less intermediate

deformation as the drops are' just torn apart'. Consequently the shear viscosity is stabilizing. It is for this reason that the drop sizes in homogenisers show a reduced dependency on μ_d. This variable dependency could be used to gain some insight in to the nature of drop breakage in rotor stators.

The viscosity seems to play an important part in determining the droplet size distribution. Higher viscosities lead to wider distributions. The relative influence of viscosity in stabilizing the drop also helps determine whether the breakup mechanism involves breaking through a stretching mechanism or shattering.

2.4.8. Dispersion in pipes

In order to model the recycle loop it is important to understand under what conditions it is reasonable to neglect the dispersive forces in the pipes. Sleicher (1962) claims that the correlation developed by Hinze in Equation 2.20 does not apply to dispersion in pipes. The biggest problem with this work is the method used to determine $d_{\max}$. The initial drops were mono-disperse i.e. all of the same size. For a given velocity an initial drop size was determined for which 20% of the drops broke up in the pipe. This contradicts the assertion that the pipe length was long enough for equilibrium to be reached. Evidence from stirred tank experiments show that equilibrium can take hours to reach (Calabrese 1986a). In Sleicher's experiment the residence time in the pipe was 2.8 seconds. Also the same stirred tank experiments show that $d_{\max}$ can be very much larger that the median drop diameter. So Sleicher's method is unlikely to be a true measure of $d_{\max}$. Since his experiment is not at equilibrium and he is not truly correlating $d_{\max}$ it is not surprising that the equations derived by Hinze (1955) do not apply. For the present work it is not necessary to precisely determine the maximum stable drop size in the pipe. It is necessary only to try and eliminate drop breakup in the pipework. The literature seems uncertain about which exact correlation to use. However a comparison of the order of magnitude of the Reynolds numbers in the tank and in the pipe should clearly show which region will have the largest stable drop size and confirm whether it is reasonable to ignore the possibility of breakup in the pipes.

2.5. Analysing drop size distributions

All the theoretical models derive relationships for the maximum stable drop size. Many product properties are more closely related to the Sauter mean diameter. Consequently one of the main preoccupations with the drop size distribution is determining the relationship between the two. The majority of work finds that they are proportional but this is disputed.

For characterising the inline mixer it is important to know when this relationship can be applied and when it is inappropriate.

It has been observed experimentally that the Sauter mean diameter, d_{32}, is proportional to the maximum stable drop size. The former is often used instead since it is easier to measure (Brown and Pitt 1972). The validity of this substitution is questioned but there is good experimental evidence to support it. A study of viscous droplets found $d_{32} \approx 0.6 d_{\max}$ (Calabrese et al 1986a). Although the constant of proportionality appeared to decrease somewhat as the viscosity increased. Experiments on a non-coalescing Kerosene in water emulsion showed a very good fit for the relationship $d_{32} \approx 0.7 d_{\max}$ (Brown and Pitt 1972).

The theoretical basis for this proportional relationship has been attacked (Pacek et al 1998) and consequently the validity of correlating d_{32} number by Weber is also questioned. Pacek assumes that drops break in two and that therefore the drop size distribution should be a log normal frequency distribution. Observations by other workers show that drops can shatter in to many pieces (Chang et al 1981) so this assumption seems overly restrictive. Even allowing for this there are other problems with the analysis. The lognormal distribution is used to calculate d_{32} as a function of both $d_{\max}$ and $d_{\min}$ using Equation 2.35. The relationship given is that,

Equation 2.31

$$d_{32} \approx \frac{0.5\left(d_{\max} + d_{\min}\right)\left((m+1)^2 + 0.443(m-1)^2\right)}{(m+1)^2 + 0.148(m-1)^2}$$

Where $m = {d_{\max}}/{d_{\min}}$. This is indeed a nonlinear function of $d_{\max}$ but as $m \to \infty$ then it reduces to $d_{32} \approx 0.63 d_{\max}$ which is in very good agreement with the experimental findings of Calabrese et al (1986a) and within 10% of the value found by Brown and Pitt (1971). The experimental system studied by Pacek produced values of $m \approx 10$ because of coalescence. In this case it is not surprising that he finds drop size is not correlated by

Equation 2.37 since the correlation is valid for non coalescing systems. Systems without coalescence typically show values of $m \approx 80$ (Calabrese et al 1986a). Provided coalescence is not significant, or equivalently that $d_{\max} >> d_{\min}$, then the objection of Pacek et al (1998) can be dismissed.

One theoretical justification (Chen and Middleman 1967) for this relationship between $d_{\max}$ and d is explicit in using Kolmogorov's -5/3 spectrum. Consequently it is not clear whether it will be valid in cases where isotropic turbulence is not the mechanism of droplet breakup. Chen and Middleman (1967) assume that there is a probability of a drop of diameter d existing at equilibrium. They further assume that this probability is a function of the ratio of turbulent energy to surface energy. The surface energy $\approx \sigma d^2$. If the drop absorbs energy from eddies smaller than itself then the energy absorbed is given by the product of the drop volume with the energy density in this part of the spectrum i.e.

Equation 2.32

$$\rho_c d^3 \int_{1/d}^{\infty} E(k)dk$$

Using these assumptions and substituting the Kolmogorov spectrum in to Equation 2.23 they find that the probability of a drop surviving is given by,

Equation 2.33

$$p(d) = p\left(\frac{\rho_c}{\sigma}\varepsilon^{2/3} d^{5/3}\right)$$

Equation 2.21 can be used to substitute for ε which then gives,

Equation 2.34

$$p(d) = p\left(\frac{d}{D} We^{0.6}\right)$$

This expression is then identified as the probability density function describing the droplet size distribution. This can be used to calculate the Sauter mean diameter which is defined,

Equation 2.35

$$d_{32} = \frac{\int_0^{\infty} d^3 p(d)\ dd}{\int_0^{\infty} d^2 p(d)\, dd}$$

By making the substitution $\xi = \frac{d}{D} We^{-0.6}$ the integral becomes,

Equation 2.36

$$d_{32} = DWe^{-0.6} \frac{\int_0^\infty \xi^3 p(\xi)\ d\xi}{\int_0^\infty \xi^2 p(\xi)\, d\xi}$$

Or more simply that,

Equation 2.37

$$\frac{d_{32}}{D} \propto We^{-0.6}$$

Comparison between Equation 2.37 and Equation 2.23 then proves that the Sauter mean drop size is proportional to the maximum stable drop size. This result is confirmed by experiment but this argument by Chen and Middleman (1967) is not entirely consistent with Hinze's theory. The problem lies in identifying the probability of a drop breaking (Equation 2.34) with the probability density function of the drop size distribution used in Equation 2.35. A non coalescing system is implicitly assumed in their study. So drops larger than the stable size limit will have broken up at equilibrium. Consider the breakup of drops slightly larger than this limit. They may breakup in to many small fragments (consistent with observations (Ali et al 1981, Chang et al 1981)). Then these smaller drops will be below the maximum stable drop size and not suffer further breakage. The number density of drops at this small size then clearly depends on the probability of them being created as daughter drops and not on their own stability. There is no reason why the daughter droplet distribution should be a function of the turbulent spectrum at the scale of the daughter droplets. The turbulent spectrum at the scale of the parent drop may play a part but that is not what Chen and Middleman (1967) are arguing. Another example might make this point clearer. Equation 2.34 is consistent with Hinze's theory. From this theory though we can see that p(d) takes only one of two values: either $d > d_{\max}$ in which case p(d) = 0, the drop cannot survive and will break; or $d < d_{\max}$ and p(d) = 1, the drop is stable and will not break. Clearly then it is not possible to identify this probability with the PDF of the drop size distribution.

There is a result that shows this effect very clearly. Ruiz et al (2002) investigated a dilute dispersion of inviscid drops. The authors raised the temperature from 22 to 32 $^{\circ}C$ and observed that d_{32} fell. They attributed this to a lowering of the interfacial tension that decreased stability. This is certainly true but it is interesting to look more closely at the change in the drop size distribution. There was a small but noticeable decrease in $d_{\max}$ but a much larger increase in the quantity of the smallest drops. This change of droplet size distribution is very good evidence to undermine the argument of Chen and Middleman (1967). If Equation 2.33 is true then a change in σ should simply cause the distribution to transform according to a contraction along the axis representing diameter. This is not observed and the shape of the distribution is changed.

The proportionality between maximum and mean drop size can still be reconciled with Hinze's theory but it requires a different assumption. If it is assumed that the observed droplet size distribution is a function of $d/d_{\max}$ then Equation 2.34 will be true for the drop size distribution since $d_{\max}$ is determined by $DWe^{-0.6}$. The substitution in to Equation 2.35 can then still be made and the same result recovered. It has been shown experimentally that the drop size distribution can indeed be normalized by the $d_{\max}$ in this manner (Calabrese et al 1986b). This normalised distribution may become narrower as impeller speed is increased (Stamatoudis and Tavlarides 1981).

So provided that there is no coalescence then the relationship between d_{32} and $d_{\max}$ does not require isotropic turbulence as claimed in the literature. Consequently it could be applied to rotor stators where the turbulence might not be isotropic.

2.6. Population Balances

Population balances are a method for analysing the transitional drop size distribution during mixing. This approach has been applied to dispersion in stirred tanks to help characterise the process. It is hoped that these methods can also be used to describe dispersion in rotor-stators. A quick overview of the work that has been done for stirred tanks will show how it could be extended to include rotor stators.

The PDF for the drop size distribution as a function of drop diameter, *d*, is $f_1(d)$. The rate of change of the distribution is given by (Ramkrishna 2000),

Equation 2.38

$$\frac{df_1(d)}{dt} = -b(d)f_1(d) + \int_d^\infty v(d')b(d')P(d|d')f_1(d')dd'$$

$b(d)$ is the breakage frequency and coalescence has been ignored. The first term on the right hand side represents the losses as drops of diameter *d* break up. The integral gives the increase as larger drops break up to form drops of diameter *d*. $v(d')$ is the number of daughter droplets that form and $P(d|d')$ is the probability of producing a daughter droplet of size *d* from a parent of size *d'*.

Experimental observations are made of the change in the drop size distribution giving the left hand side of Equation 2.38. The inverse problem is to find the breakage frequency and daughter droplet distribution. This is not straightforward since many combinations of breakage functions and daughter droplet distributions can produce the same observed change.

The method most often used in the literature is to assume that the size of the daughter droplets is related to the size of the parents. This gives that (Ramkrishna 2000),

$$P(d|d') = P\left(\frac{d}{d'}\right)$$

This leads to a self similar form for the drop size distribution which can be described as a function of $d^\alpha t$ and the solution to Equation 2.38 becomes more tractable. There are many studies that verify the validity of this assumption (Ramkrishna 1973, Sathyagal et al 1996, Narsimhan et al 1984). However the method of solution still requires some assumptions to be made about the forms of the breakage functions and daughter droplet distributions. There seem to be as many assumptions as there are studies. The breakage function is often expressed as an exponentially increasing function of drop size and the exponent is fitted to match the observed data (Ramkrishna 1973). However not all studies agree that a power law is most appropriate (Sathyagal 1996). Although this might not be too serious a problem: the evolution of the drop size distribution is insensitive to the exact form of the breakage function (Ruiz and Padilla 2004). On the other hand Ruiz and Padilla (2004) did find that the daughter droplet distribution had a big effect on the resulting drop size distribution. In their study they assumed a U-shaped distribution of daughter drops with the lowest probability corresponding to producing two equally sized drops. The implicit assumption is that the drop splits in to two. Other assumptions for the form of the

daughter droplet distribution include uniform or perfectly random (Narsimhan et al 1979), a beta distribution (Narsimhan et al 1984) and normally distributed. Sathyagal et al (1996) applied several models to the same system and found very different results for the daughter droplet distribution in each case.

Population balances can be applied to characterise the dispersion process. In order to be able to solve the equations the process must be self similar. And even then assumptions about the answer must be made which can prejudice the result. For self similarity to be valid in rotor-stators it is necessary that the size of the daughter droplets be related to the size of the parents.

2.7. Summary

To model the effect of the recycle loop volume its properties as a mixing field must be identified and related to the other sections of the system. The experimental method of Hinze (1993) allows the predictions of the model to be evaluated but there are several factors that could be changed to make the procedure more rigorous. All the materials and equipment can be assessed in relation to any assumptions that need to be made for the model. Many of the methods to characterise dispersive processes assume isotropic turbulence. It has been shown that the conclusions do not actually require this statistical form for the disruptive force. In order to apply the standard correlations to the maximum drop size it is only required that the dimensional analysis is appropriate i.e. that there are no other variables influencing the process. To use the Sauter mean in correlations it is necessary that the daughter droplet size is related to the parent drop size so that the Sauter mean is proportional to the maximum stable drop size. The same condition applies to using the population balance models to describe the process.

3. Modelling the recycle loop volume

The primary aim of this present work is to understand the effect of the recycle loop volume in batch recirculation emulsification. To do this some general assumptions about the processes that occur in the recycle loop have been made. The relevant mass balances have been set up and solved analytically and numerically for particular cases. In addition the model of Baker (1993) has been extended to include semi-batch operations where the tank volume changes with time. This has particular relevance to laboratory scale experiments where the taking of samples produces a relatively large change in the liquid volume. Some aspects of the experimental procedure required the distributive mixing throughout the recycle loop and tank to be modelled. Finally the models have been applied to some illustrative examples to indicate the significance of the findings.

3.1. General assumptions

In general there are many processes that can occur in the pipelines to alter the product. Most of these have been neglected for this present worl. It has been assumed that there is no coalescence, no droplet breakup and no evolution of the interfacial tension in the recycle loop. The intense mixing field of the inline mixer ensures that the droplets will be smaller than the maximum stable drop in the pipes so the assumption of no droplet breakup is valid. The condition that there be no coalescence restricts the model to situations with very low dispersed phase fraction or that are stabilised by surfactant. As noted in the literature review the evolution of interfacial tension with time is eliminated at high surfactant concentrations. Therefore a situation where it can be ignored is realistically achievable. The only remaining effect of the recycle loop volume is that it determines a finite period of time during which a fluid element is not distributively mixed in the tank or dispersed in the inline mixer. In the context of mixing field theory it is essentially a field with zero mixing intensity but a finite residence time. The precise nature of the effect depends on the physical arrangement of the system and the flow regime in the pipes.

3.2. Plug flow in the recycle loop

The particular arrangement that has been considered is shown in Figure 3.1. The stirred tank has liquid volume V and the recycle loop has volume ζ. The inline mixer is located at the beginning of the recycle loop and its volume is included in ζ. The flowrate round the recycle loop is F and time $t = 0$ is set at the moment the inline mixer is started. The fluid is already flowing round the system at $t = 0$ so the recycle loop is fully charged with

fluid. The initial condition is that none of the material in the tank has been exposed to the high shear of the inline mixer, i.e. $C_0 = 1$. The same notation as Baker (1993) is used where C_i is the volume fraction in the tank that has passed *i* times through the high shear mixing field of the inline mixer. C'_i is the volume fraction of the material returning to the tank that has passed through the inline mixer *i* times.

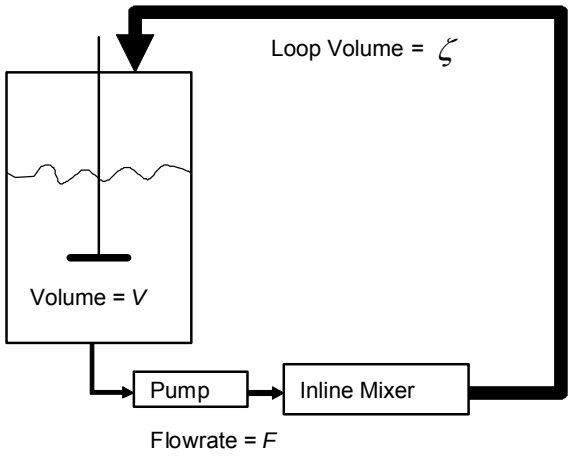

Figure 3.1 Schematic diagram of the system being modelled.

At industrial and pilot plant scales the flow in the pipes will likely be turbulent. This can be modelled as plug flow. This assumes that every fluid element has a residence time of ζ/F in the recycle loop. Once material C_i flows out of the tank at time *t* it passes through the inline mixer. At time $t + \zeta/F$ it is then returned to the tank as C'_{i+1}. This leads to the identification that,

Equation 3.1

$$C'_i(t) = C_{i-1}\left(t - \zeta/F\right)$$

This has been used to establish the population balances for the stirred tank. These are most easily understood by considering the behaviour in distinct periods of time.

3.2.1. Specific analytical solutions

$0 < t < \zeta/F$

During this period the fluid returning from the recycle loop has not been subject to the dispersive mixing field and has the same composition as the fluid in the tank. The mass balance can then be expressed as,

Equation 3.2

$$\frac{dC_i}{dt} = 0$$

The boundary condition is used to get the solutions,

Equation 3.3

$$C_0(t) = 1$$
$$C_i(t) = 0\,,\ i > 0$$

$\zeta/F < t < 2\zeta/F$

Between these times the material entering the tank has passed through the inline mixer so $C'_0 = 0$. The mass balance on C_0 is then given by,

Equation 3.4

$$\frac{dC_0}{dt} = -\frac{F}{V}C_0$$

The boundary condition is that C_0 must be continuous at $t = \zeta/F$ so the solution is,

Equation 3.5

$$C_0(t) = e^{-\frac{F}{V}(t-\zeta/F)}$$

Equation 3.4, and hence its solution Equation 3.5, is valid for all $t > \zeta/F$. The mass balance on C_1 is,

Equation 3.6

$$\begin{aligned}\frac{dC_1}{dt} &= -\frac{F}{V}\left(C_1(t) - C'_0(t)\right) \\ &= -\frac{F}{V}\left(C_1(t) - C_0\left(t - \zeta/F\right)\right) \\ &= -\frac{F}{V}\left(C_1(t) - 1\right)\end{aligned}$$

Equation 3.3 has been used to substitute for C_0. The boundary condition that $C_1\left(\zeta/F\right) = 0$ leads to the solution,

Equation 3.7

$$C_1(t) = 1 - e^{-\frac{F}{V}\left(t - \zeta/F\right)}$$

A shortcut to this solution is found by noting that no material has had time to pass through the recycle loop more than once so $C_i = 0$ for i >1. The volume fractions must sum to 1

so $C_1(t) = 1 - C_0(t) = 1 - e^{-\frac{F}{V}\left(t - \zeta/F\right)}$.

$\underline{2\zeta/F < t < 3\zeta/F}$

At the start of this period the equation describing C_0 changes from Equation 3.3 to Equation 3.5. So in this period $C'_1(t) = C_0\left(t - \zeta/F\right) = e^{-\frac{F}{V}\left(t - 2\zeta/F\right)}$. This affects the mass balance on C_1 which becomes,

Equation 3.8

$$\frac{dC_1}{dt} = -\frac{F}{V}\left(C_1(t) - e^{-\frac{F}{V}\left(t - 2\zeta/F\right)}\right)$$

The general solution is,

Equation 3.9

$$C_1 = \frac{F}{V}\left(t + K_1\right)e^{-\frac{F}{V}\left(t - 2\zeta/F\right)}$$

C_1 must be continuous at $t = 2\zeta/F$ so the particular solution is,

Equation 3.10

$$C_1 = \frac{F}{V}\left(t + \frac{V}{F}\left(1 - e^{-\zeta/V}\right) - 2\zeta/V\right)e^{-\frac{F}{V}\left(t - 2\zeta/F\right)}$$

In this period there cannot be any material which has been recycled more than twice so it is easiest to express C_2 as,

Equation 3.11

$$C_2 = 1 - C_0 - C_1$$

$$C_2 = 1 - e^{-\frac{F}{V}\left(t - \zeta/F\right)} - \frac{F}{V}\left(t + \frac{V}{F}\left(1 - e^{-\zeta/V}\right) - 2\zeta/V\right)e^{-\frac{F}{V}\left(t - 2\zeta/F\right)}$$

3.2.2. General form of solutions

These specific examples show that the general mass balance on C_i is,

Equation 3.12

$$\frac{dC_i(t)}{dt} = -\frac{F}{V}\left(C_i(t) - C_{i-1}\left(t - \zeta/F\right)\right)$$

And the solution is in two parts, for $t < (i+1)\zeta/F$ then it is given by,

Equation 3.13

$$C_i = 1 - \sum_{k=0}^{i-1} C_k$$

Starting with the solution for C_0 in Equation 3.5 it can be proved by induction that the solution for $t > (i+1)\zeta/F$ is given by,

Equation 3.14

$$C_i = \left(\frac{F}{V}\right)^i f_i(t) e^{-\frac{F}{V}\left(t - (i+1)\zeta/F\right)}$$

$f_i(t)$ is found using the mass balance Equation 3.12 which gives the relationship,

Equation 3.15

$$\frac{df_i(t)}{dt} = f_{i-1}\left(t - \zeta/F\right)$$

The constant of integration is found from the condition that $C_i(t)$ must be continuous at $t = (i+1)\zeta/F$. These analytical expressions rapidly become increasingly cumbersome as *i* increases. Baker (1993) showed that for many mixers most of the effect occurs on the first pass. Therefore exact analytical solutions are not necessary for large values of *i* and only the first three are given here. For C_0 the solution is,

Equation 3.16

$$C_0(t) = 1 \qquad ,t \le \zeta/F$$
$$C_0(t) = e^{-\frac{F}{V}(t-\zeta/F)} \qquad ,t \ge \zeta/F$$

For C_1 the solution is,

Equation 3.17

$$C_1(t) = 0 \qquad ,t \le \zeta/F$$
$$C_1(t) = 1 - e^{-\frac{F}{V}\left(t-\zeta/F\right)} \qquad ,t \le 2\zeta/F$$
$$C_1 = \frac{F}{V}\left(t + \frac{V}{F}\left(1 - e^{-\zeta/V}\right) - 2\zeta/V\right)e^{-\frac{F}{V}\left(t-2\zeta/F\right)} \qquad ,t \ge 2\zeta/F$$

And the volume fraction in the tank that has passed through the loop twice is given by,

Equation 3.18

$$C_2(t) = 0 \qquad ,t \le 2\zeta/F$$
$$C_2(t) = 1 - e^{-\frac{F}{V}\left(t-\zeta/F\right)} - \frac{F}{V}\left(t + \frac{V}{F}\left(1 - e^{-\zeta/V}\right) - 2\zeta/V\right)e^{-\frac{F}{V}\left(t-2\zeta/F\right)} \qquad ,t \le 3\zeta/F$$
$$C_2(t) = -\left(\frac{F}{V}\right)^2\left[\frac{t^2}{2} + \left(\frac{V}{F}\left(1 - e^{-\zeta/V}\right) - 3\frac{\zeta}{F}\right)t + \frac{9}{2}\left(\frac{\zeta}{F}\right)^2 - 3\frac{\zeta V}{F^2}\left(1 - e^{-\zeta/V}\right) + \left(\frac{V}{F}\right)^2\left(1 - \left(1 + \frac{\zeta}{V}\right)e^{-\zeta/V}\right)\right]e^{-\frac{F}{V}\left(t-2\zeta/F\right)} \qquad ,t \ge 3\zeta/F$$

It is worth noting that as $\zeta \to 0$ these solutions recover the Poisson distribution derived in Baker (1993) for negligible recycle loop volume.

3.2.3. Numerical solution

For larger values of *i* the mass balances have been solved numerically by applying a simple forward difference algorithm to Equation 3.12. The numerical equation is,

Equation 3.19

$$C_i(t+\Delta t) = C_i(t) - \frac{F}{V}\left(C_i(t) - C_{i-1}\left(t - \zeta/F\right)\right)\Delta t$$

The success of the implementation was confirmed by comparison with the analytical solutions above and also by checking that the solution of Baker (1993) was recovered in the limit $\zeta \to 0$.

3.3. Laminar flow in the recycle loop

At the laboratory scale the flowrates can be small and the regime in the pipes may be laminar. In this case the problem is more complicated since the fluid velocity varies across the pipe. For a pipe of radius *a* the axial velocity at a radius *r* is given by

Equation 3.20

$$u(r) = u_0\left(1 - r^2/a^2\right)$$

The peak flow velocity, u_0, is given by,

Equation 3.21

$$u_0 = 2F/\pi a^2$$

Equation 3.20 can be used to calculate the volumetric flowrate *F** in an annulus between two radii r_1 and r_2.

$$F^* = \int_{r_1}^{r_2} 2\pi u_0\left(1 - r^2/a^2\right) r\, dr$$

$$F^* = 2\pi u_0\left[\frac{r^2}{2} - \frac{r^4}{4a^2}\right]_{r_1}^{r_2} = \pi u_0\left(r_2^2 - r_1^2 + \frac{r_1^4 - r_2^4}{2a^2}\right)$$

The average residence time, Δt, in this annulus can be determined by,

Equation 3.22

$$\Delta t = \frac{Volume}{Flowrate} = \frac{\zeta}{2F}\left(\frac{r_2^2 - r_1^2}{r_2^2 - r_1^2 + \frac{r_1^4 - r_2^4}{2a^2}}\right)$$

ζ is the total volume of the pipe and F is the total flowrate through the pipe. To capture the effect of the varying velocities the pipe was divided up in to ten such annular regions, each of equal volumetric flowrate. Each annulus was then considered to be a separate recycle loop described by a single residence time. The properties of each section are shown Table 3.1.

Inner Radius / a	Outer Radius / a	Residence time / (ζ/F)
0.000	0.226	0.513
0.226	0.325	0.543
0.325	0.405	0.578
0.405	0.475	0.621
0.475	0.542	0.675
0.542	0.606	0.747
0.606	0.672	0.847
0.672	0.744	1.005
0.744	0.827	1.311
0.827	1.000	3.164

Table 3.1 Showing the descriptions of the annular sections of laminar flow

So with ten separate recycle loops, each of volumetric flowrate $0.1F$ then the general mass balance becomes,

Equation 3.23

$$\frac{dC_i(t)}{dt} = -\frac{F}{V}\begin{pmatrix} C_i(t) - 0.1C_{i-1}\left(t - 0.513\zeta/F\right) - 0.1C_{i-1}\left(t - 0.543\zeta/F\right) - 0.1C_{i-1}\left(t - 0.578\zeta/F\right) \\ - 0.1C_{i-1}\left(t - 0.621\zeta/F\right) - 0.1C_{i-1}\left(t - 0.675\zeta/F\right) - 0.1C_{i-1}\left(t - 0.747\zeta/F\right) \\ - 0.1C_{i-1}\left(t - 0.847\zeta/F\right) - 0.1C_{i-1}\left(t - 1.005\zeta/F\right) - 0.1C_{i-1}\left(t - 1.311\zeta/F\right) \\ - 0.1C_{i-1}\left(t - 3.164\zeta/F\right) \end{pmatrix}$$

Exceptions need to be made for C_0 and C_1. For C_0 the identity $C'_i(t) = C_{i-1}(t - \Delta t)$ does not hold. For each annular segment the particular residence time Δt needs to be taken in to account to give,

Equation 3.24

$$C'_0(t) = 1,\ t \le \Delta t$$
$$C'_0(t) = 0,\ t \ge \Delta t$$
$$C'_1(t) = 0,\ t \le \Delta t$$
$$C'_1(t) = C_0(t - \Delta t),\ t \ge \Delta t$$

Equation 3.23 has been solved numerically using the same approach expressed in Equation 3.19.

3.4. Combining pipe sections.

In the experimental system several pipes were connected to make a large recirculation loop. Where two pipes with laminar flow are connected in series then they have been assumed to behave as one pipe. The fluid is incompressible and streamlines do not cross so an element in the outer annulus of the first pipe will pass through the join and will end up in the outer annulus of the second pipe. The flow in the narrow join may be turbulent but turbulent radial mixing is achieved over a length of 100 pipe diameters (Etchells and Meyer 2004). Provided the join is short then this will be a reasonable assumption to treat them as one pipe.

A laminar section connected in series to a turbulent section has been modelled by combining the two results. Ten residence times are found for the laminar section and on to each is added the uniform residence time of the turbulent section.

3.5. Adaptations for Semi-Batch Operation

In the laboratory samples were taken from the tank and the volume dropped. This effect was included in the model by allowing V to vary with time. If ten samples were taken, 1 every 2 minutes, and the total volume dropped by 0.5 l then V was modelled as decreasing in 50 ml increments every 2 minutes. Equation 3.23 and Equation 3.19 were both solved numerically in MS Excel. In this environment it is straightforward to evaluate V separately at each time step.

3.6. Distributive Mixing

When preparing the emulsions the aqueous phase was present in the tank and recycle loop when the oil phase was added to the tank. It was necessary to calculate the distributive

process to ensure a uniform distribution of oil was achieved before the mixer was started. In this case the mass balance on the volume fraction of oil in the tank, ϕ, is given by,

Equation 3.25

$$\frac{d\phi(t)}{dt} = -\frac{F}{V}\left(\phi(t) - \phi\left(t - \zeta/F\right)\right)$$

Equation 3.25 applies to turbulent flow. For laminar flow the same adjustment may be made as before. The initial condition is that,

Equation 3.26

$$\phi(t) = 0 \quad , t < 0$$
$$\phi(t) = \phi_0 \quad , t = 0$$

The solution was found numerically using the same approach expressed in Equation 3.19.

3.7. Examples

Some example calculations have been made to assess the characteristic predictions of this model that differ from the literature. When comparing the predictions of the Baker (1993) model with this extension it is necessary to address an ambiguity. In Baker's model the tank volume and the total volume are the same. In this extended model they are different. Baker defines the number of batch volumes by,

Equation 3.27

$$N_{BV} = \frac{Ft}{V}$$

For the extended model a decision needs to be made whether it is more appropriate to use the total volume, $V + \zeta$, or just the tank volume, V, when calculating *N*. It was decided that total volume is more appropriate. The issue is best understood by considering an example. A system has a recycle loop of volume 0.1 l. The user charges 3.5 l of fluid to the tank. If he neglects the recycle loop volume and applies the Baker (1993) model he will calculate the number of batch volumes by,

Equation 3.28

$$N_{BV} = \frac{Ft}{3.5l}$$

To make a fair comparison with the extended model it is important to compare values at the same time. If N is defined as ,

Equation 3.29

$$N_{BV} = \frac{Ft}{V + \zeta}$$

Then points at the same time will be translated to the same value of N (since $V + \zeta$ =3.4+0.1). This is consistent with Equation 3.27 because in Baker's model $\zeta = 0$.

3.7.1. Characteristic profile

The fraction of material that has not passed through the inline mixer is very important in determining the properties of the end product. Values of V, ζ and F were chosen as 3.5 l, 3 l, and 1 l min^{-1} as an example relevant to the laboratory scale experiments. The resulting profiles of C_0 for the different models are shown in Figure 3.2.

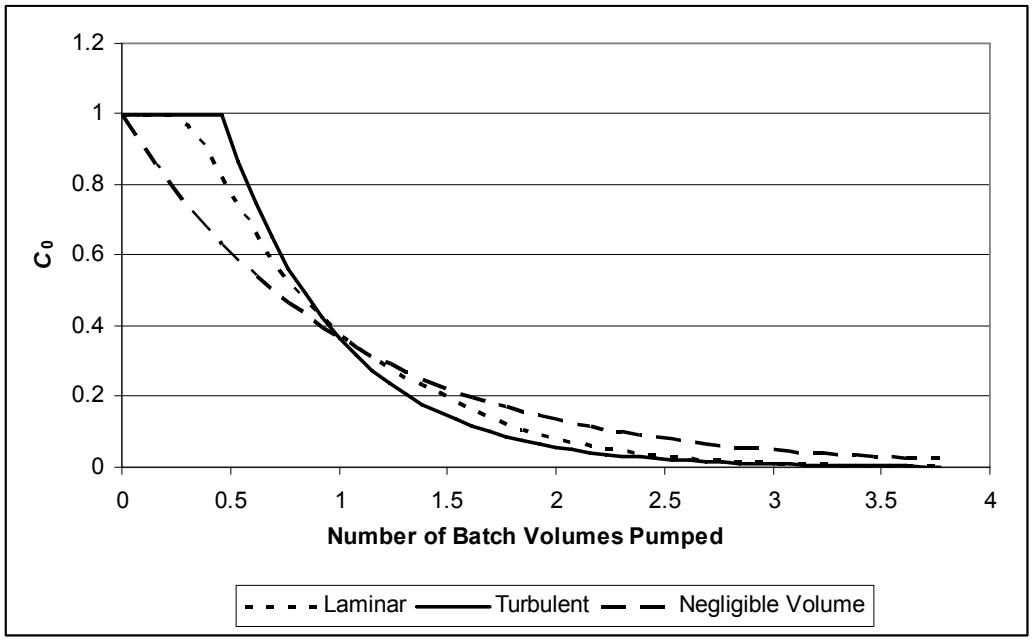

Figure 3.2 Comparing the Evolution of C_0 Predicted by Different Models.

Figure 3.2 shows that in the case of turbulent flow there is a period of delayed response but then C_0 drops more quickly than predicted by the model of Baker (1993) which assumed a

negligible recycle loop volume. If the flow in the pipes is laminar then some fluid elements have a shorter residence time than for the turbulent case. This reduces the disagreement with the Baker (1993) model. Nevertheless there is still a clear, characteristic prediction of a delay followed by a sharper drop than would be expected from the standard model of Baker (1993). For very low values of C_0 the relative difference between the models becomes more pronounced. After 3 batch volumes have been pumped the laminar and turbulent flow models both predict that $C_0 \approx 1\%$. The Baker (1993) model predicts that $C_0 \approx 5\%$.

3.7.2. Narrower drop size distribution

The second key feature of this extended model is that it predicts a narrower distribution of C_i in the tank. For the same example the distribution of C_i after 1 batch volume (6.5 l) has been pumped is shown in Figure 3.3

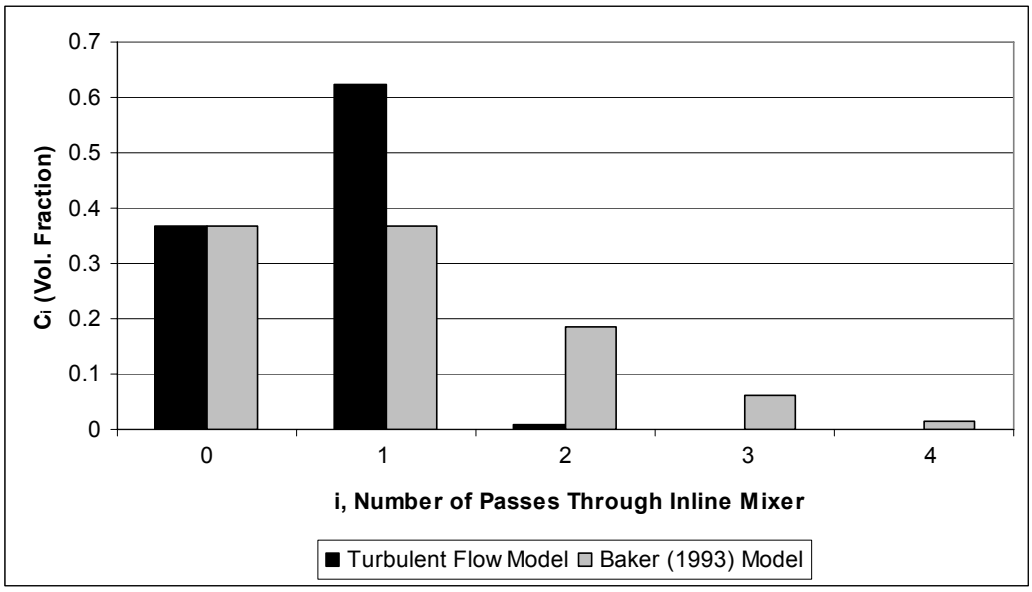

Figure 3.3 Comparing predicted distributions of C_i for different models.

The Poisson distribution of Baker (1993) clearly overpredicts the amount of material that will pass more than once through the recycle loop. This suggests that experiments at laboratory scale will be able to achieve narrower distributions than those possible at industrial scale.

3.7.3. Impact on scale up calculations

This example exaggerated the size of the recycle loop volume as a proportion of total volume in order to more easily identify the nature of the effect. For more realistic proportions the differences will be smaller. However very small differences can have a

significant impact on the success of scale up. Consider a product specification requiring 99.5 % of the material to pass through the inline mixer. At pilot scale the recycle loop might be 15% of the total batch volume, B_V. Substituting $\zeta = 0.15 B_V$ and $V = 0.85 B_V$ in to Equation 3.16 and applying the product specification gives,

Equation 3.30

$$C_0(t) = e^{-\frac{F}{0.85B_v}(t-0.15B/F)} = 0.005$$
$$\frac{Ft}{B_V} \equiv N_{BV} = 0.15 - 0.85\ln 0.005 = 4.65$$

So pilot plant trials would report that specification is reached after 4.65 batch volumes are pumped. Upon scale up to industrial scale (where Baker's assumption of negligible volume is appropriate) then the fraction C_0 is given by,

Equation 3.31

$$C_0 = e^{-N_{BV}} = e^{-4.65} = 0.01$$

So in fact only 99 % of the material will have passed through the mixer: the batch will be off specification. In fact to reach specification the required value of N_{BV} is,

Equation 3.32

$$N_{BV} = -\ln 0.005 = 5.3$$

This represents an increase of nearly 14% in the production time. Errors of this magnitude could have a big impact on the profitability of a process.

Applying the same ideas it is possible to derive a general expression for the ratio between the required number of batch volumes at pilot scale and at industrial scale:

Equation 3.33

$$\frac{N_{BV}(Pilot)}{N_{BV}(Industry)} = 1 - x\left(1 + \frac{1}{\ln C_0}\right)$$

x is the recycle loop volume as a fraction of the total batch volume in the pilot plant. C_0 is the value required by the product specification. So in the previous example the calculation would be,

Equation 3.34

$$\frac{N_{BV}(Pilot)}{N_{BV}(Industry)} = 1 - 0.15\left(1 + \frac{1}{\ln 0.005}\right) = 0.878$$

Clearly this only applies when the product specification can be stated or estimated as a required value of C_0. In cases where the specification relates to the detail of the drop size distribution then a specific investigation will need to be made.

3.7.4. The effect of decreasing tank volume

The effect of taking samples from the tank was evaluated using example variables ζ =3 l, V =3.5 l and F = 1 l min^{-1} and assuming laminar flow in the recycle loop. The tank volume was decreased by 0.05 l every 2 minutes until V=3 l. The resulting profile for C_0 was calculated and compared to the base case of constant V=3.5 l. The result is shown in Figure 3.4.

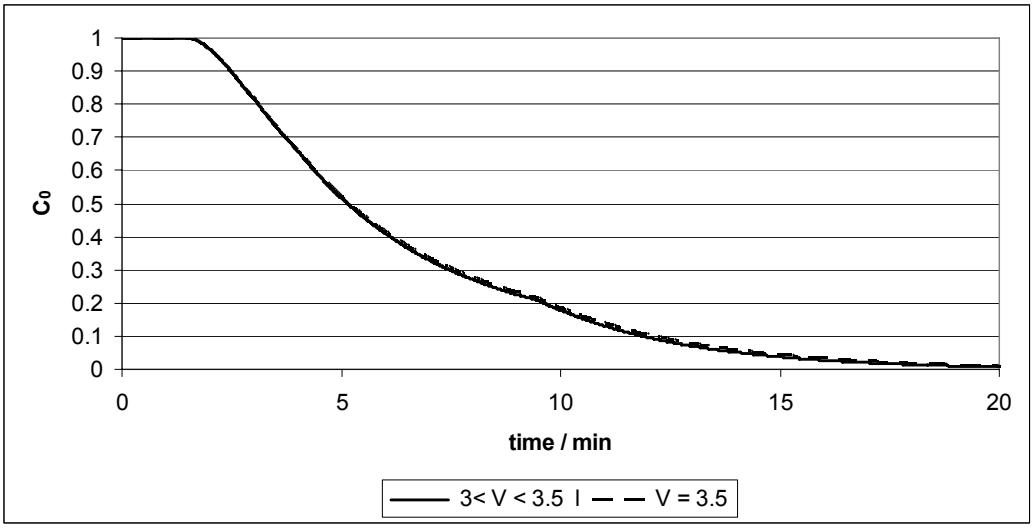

Figure 3.4 Showing the profile of C_0 over time.

Figure 3.4 shows that the change in volume produces a negligible difference in the profile of C_0. The effect on the distribution of the C_i was also captured at a time equivalent to two batch volumes being pumped. The result is shown in Figure 3.5,

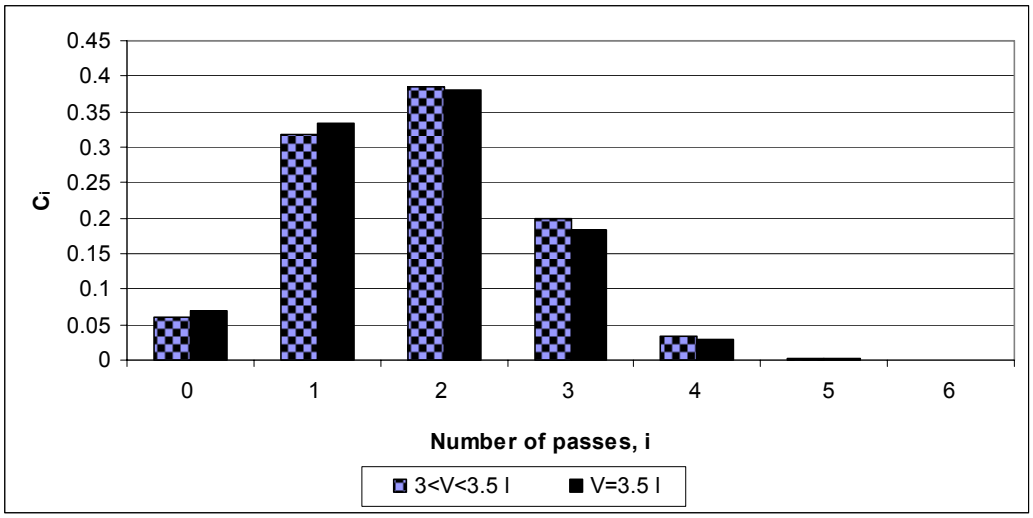

Figure 3.5 Showing the distributions of C_i at N_{BV}=2

Figure 3.5 confirms that the reduction in tank volume does not have a significant effect on the distribution of material inside the tank.

3.7.5. Distributive Mixing

The model for distributive mixing has been applied using the variables ζ =3 l, V =3.5 l, F = 1 l min^{-1} and ϕ_0 =0.1. The progress of the distributive mixing is shown in Figure 3.6.

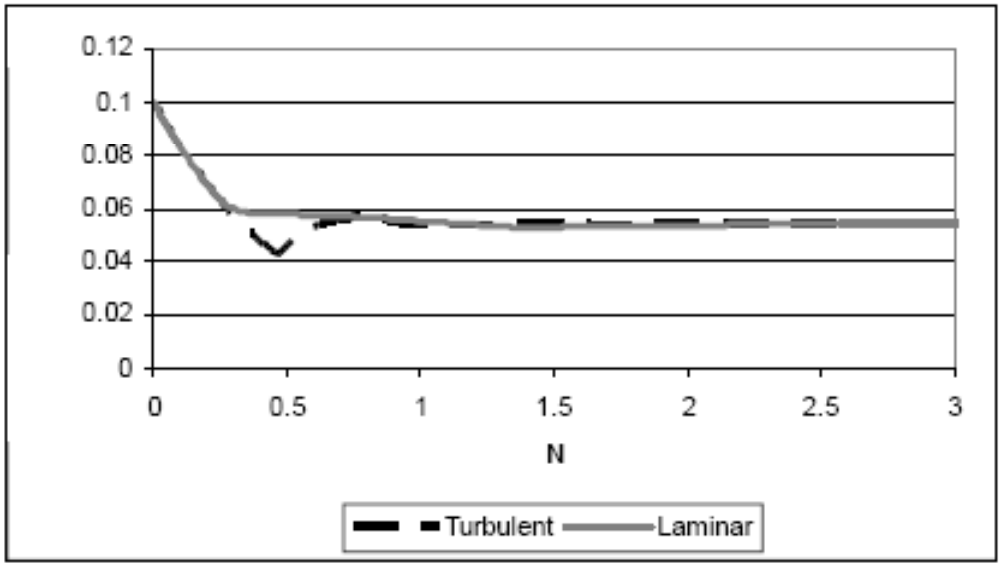

Figure 3.6 Showing the profile of ϕ with time

Figure 3.6 Shows that the concentration of oil in the tank declines with time as it is spread throughout the recycle loop. For turbulent flow in the recycle loop there is a slight oscillation in the phase fraction. For laminar flow this oscillation is damped by the

variation in residence times. In both cases the well mixed steady state is reached after approximately two batch volumes have been pumped.

3.8. A potential improvement to current industrial practice

As a final observation it is interesting to note the behaviour as the volume of the tank tends to zero. In this case the whole batch is flowing round the recycle loop in plug flow conditions. Without the backmixing effect of the stirred tank it is then possible to have exact control over the distribution of C_i: after i batch volumes have been passed round the loop the all the material will have passed i times through the inline mixer. This is a very desirable situation where close control of the droplet size distributions is important for a product, for instance in emulsion polymerisation (El-Jaby et al 2007). Unfortunately this is not a feasible setup at industrial scale. The major stumbling block is that the stirred tank is necessary for distributive mixing when the ingredients are charged to the system. There is a piece of equipment that has the potential to compromise between the attributes of a CSTR and PFR. The multistage mixing tank (Hemrajani and Tatterson 2004, p373) provides a good approximation to plug flow and is shown in Figure 3.7. It would need to be adapted to provide the necessary distributive mixing at the beginning of emulsification.

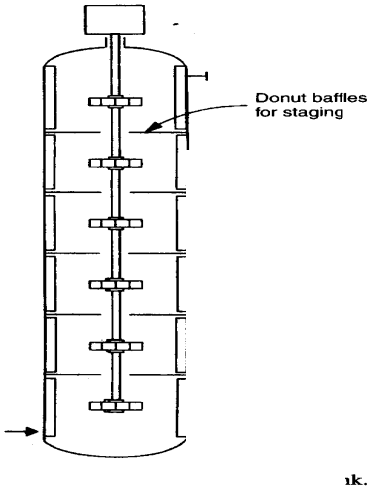

Figure 3.7 Diagram of a Multi-Stage Mixing Tank (Hemrajani and Tatterson 2004)

One possible adaptation would be to reach a compromise on the number of stages and size of the inter-stage baffle opening. More stages and smaller openings would favour plug flow whereas the opposite increases the degree of distributive mixing. Or if the aperture size could be controlled (perhaps like the shutter of an old camera) then the tank could operate as a CSTR initially and then be switched to plug flow mode when the recycle loop was operated. Alternatively the material could be charged directly in to each cell so that a

uniform initial composition was achieved. As a final suggestion the material could simply be recirculated around the recycle loop. Since plug flow is only approximated this would eventually achieve an evenly distributed mixture. All these suggestions have significant drawbacks but the potential advantages make it worth some thought. For high value products the precise control over the drop size distribution could provide a crucial commercial advantage. Production times could also be cut drastically. After one batch volume has been pumped all the material would have been through the inline mixer. By comparison with Equation 3.32 this would give a five-fold increase in production rate.

3.9. Summary

A mathematical model has been developed to explain the effects of the recycle loop volume in batch emulsification systems. The example solutions have shown the characteristics and magnitude of these effects. The extended model clearly predicts that recycle loop volume is an important consideration in the scale up stage of process development. This model also gives some insight in to the process and suggests possible ways to improve the efficiency of production by changing the mixing field in the stirred tank to promote plug flow. The predictions of the model need to be compared with experimental results to confirm its validity.

4. Modelling the effect of the inline mixer

The model of Baker (1993) gives some insight in to the operation of an inline mixer and this suggests a new way of characterising the dispersive process. Baker states that he material fraction C_i passes through the inline mixer and is returned as fraction C_{i+1}. This shows that the mixer is acting independently on each constituent of the mixture. But the separation between the constituent parts is not a physical thing. Therefore any drop size distribution can be thought of as a mixture of many mono-disperse constituents. The observed drop size distribution is discrete so there will be a finite number of these elements. The mixer can be thought of as acting on each of these components separately. If the discrete drop size distribution is expressed as a column vector then this process can be represented by a matrix transformation where,

Equation 4.1

$$[\underline{M}](\underline{x_i}) = (\underline{x}_{i+1})$$

Where $(\underline{x_i})$ and $(\underline{x}_{i+1})$ are the drop size distributions before and after passing through the mixer expressed as column vectors. $[\underline{M}]$ is the matrix transformation that represents the action of the mixer.

Solving to find the matrix is not possible without sufficient observations. If $[\underline{M}]$ is an $n \times n$ matrix then in general *n* independent observations like Equation 4.1 are necessary. In this case another $n \times n$ matrix can be constructed, $[\underline{X}_i]$ which has as its columns the *n* vectors of $(\underline{x}_i)$. By doing the same for the vectors $(\underline{x}_{i+1})$ the original matrix can be found by,

Equation 4.2

$$[\underline{M}] = [\underline{X}_{i+1}][\underline{X}_i]^{-1}$$

Unfortunately the experimental error in the measurements means that this inversion produces an answer that has very much larger errors.

The approach taken was to start with a trial solution, $[\underline{M}^*]$, and calculate the matrix of errors,

$$[\underline{M}^*](\underline{x_i}) - (\underline{x}_{i+1})$$

Then the Solver feature in MS Excel was used to vary the elements of $[\underline{M^*}]$. The target was to minimize the sum of the squared elements of the error matrix above. It is not known how close this method approaches to the real solution so the result must be compared to actual drop size distributions to assess the accuracy.

The physical properties of the transformation reduce the number of elements that need to be varied. By assuming that there is no coalescence a small drop cannot transform in to a large drop. This means the matrix must be triangular. Volume is conserved so the elements of every column must sum to 1.

The drop size distributions span about 40 of the classes of the Mastersizer output. This is too many elements for Solver to handle so neighbouring classes were merged to calculate an $18^{\times}18$ matrix.

Although this method lacks something in elegance it has the advantage that there are no a priori assumptions that feed in to it. It has the potential to develop a good intuition about the underlying process.

5. Experimental Method

An appropriate oil and surfactant were chosen to create an emulsion that would be stable and non-coalescing. The equipment used to make the emulsion consisted of a stirred tank, a peristaltic pump and an inline rotor-stator mixer. The particular items used were those that were available so initial tests were performed to establish their suitability. The experiments were performed to characterise the inline mixer's performance. This information was used to determine the distributions inside the stirred tank for comparison with both the model in the literature (Baker 1993) and the extension developed in Chapter 3.

5.1. Materials used

The dispersed phase was 350 cSt Dow Corning 200 ® series silicone oil. This was chosen because it was readily available and has been used successfully in several other studies to create oil-in-water dispersions (El-Hamouz et al 2009, El-Hamouz 2007, Calabrese et al 1986a). The specific gravity is 0.97 so the emulsions are subject to creaming. The oils in this series have varying viscosities but almost identical surface tensions with water (Calabrese et al 1986a). This makes them amenable to extending the current work to asses the effect of dispersed phase viscosity on the inline mixer's performance. This oil is very low hazard and disposal represents no risk to the environment which is a further attraction. The closed cup flashpoint is 120°C and the vapour pressure is less than 1 mmHg at room temperature so there is no need for special ventilation or extra fire risk. The LD50 (rat) is more than 2 g/kg which represents a low ingestion hazard. It is amenable to sewage treatment and in the environment it will degrade abiotically leaving inorganic silica, carbon dioxide and water. The solubility in water is very low (<100 ppb) so no allowance needs to be made to allow this process to reach equilibrium. The biggest safety hazard is the risk of slipping on a spill. Care was taken to avoid spilling and any spills were immediately mopped up.

The chosen surfactant was Texapon ® N701 manufactured by Cognis. This is a brand name for Sodium Laureth Sulfate (SLES). It was used in solution in tap water at concentration 1% by weight. Derived from natural fatty acids it has a varying chain length. Additionally it is impure and only contains 70% by weight active ingredient. For these reasons it is not generally used in academic studies. However it is commonly used in shampoos and shower gels so it has industrial relevance. Most importantly it has been shown to successfully stabilise silicone oil in water dispersions (El-Hamouz 2007, El-Hamouz et al 2009). Coalescence can be eliminated and this is an essential assumption of

the model being evaluated. Furthermore it means that samples will be stable for days (El-Hamouz 2007). To achieve this stability the concentration of SLES must be many times larger than the cmc. This needs to be true even when adsorption at the oil water interface is taken in to account. The chosen concentration was 1% by weight, as demonstrated in the literature review this is sufficient.

These materials meet all the requirements of the model to create a stable emulsion where drop size is governed only by breakage.

5.2. Equipment

A diagram of the experimental set up is shown in Figure 5.1. It shows the dimensions of the stirred tank that was used and the arrangement of the equipment.

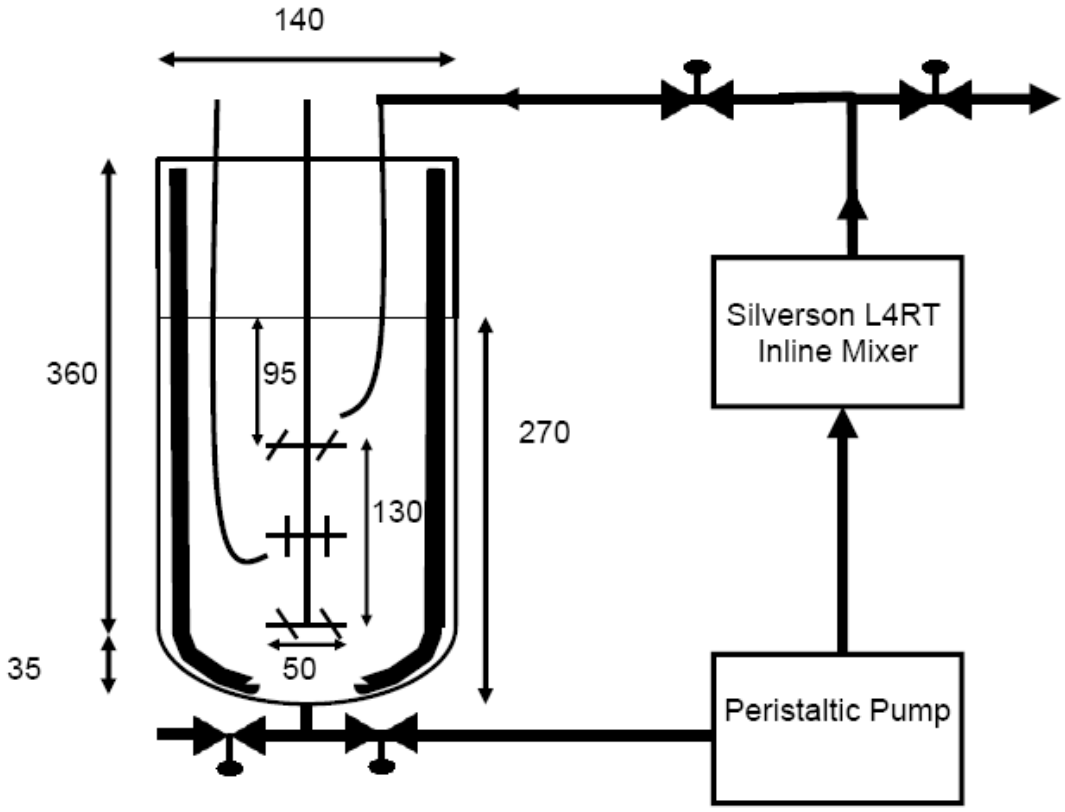

Figure 5.1 Schematic diagram of the experimental equipment. Tank dimensions in mm

5.2.1. Stirred Tank

The stirred tank was not of standard geometry. It was tall and thin, with a dished base and had an operating volume of 3.5 l. Four equally spaced baffles prevented bulk rotation of the fluid. Three co-axially mounted impellers provided the agitation. The uppermost was a down-pumping pitched blade impeller with 6 blades. The middle was a Rushton Turbine

with 8 blades. The bottom was an up-pumping pitched blade turbine with 6 blades. The blades were 12 mm deep and 2 cm long. The discs were 3.5 cm in diameter and the blades were set in to the disc so that the overall diameter was 5 cm.

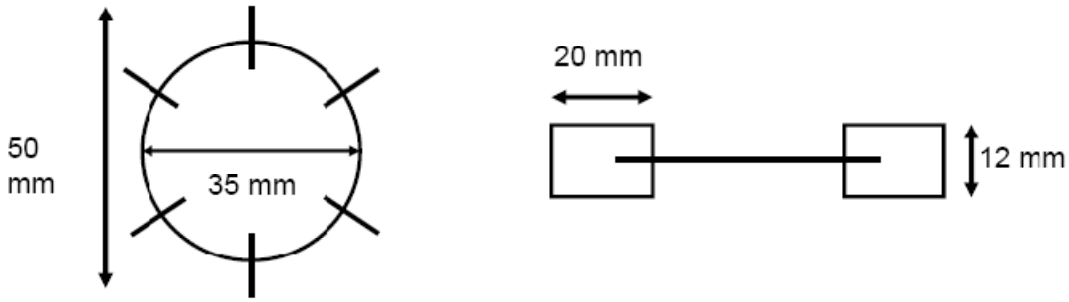

Figure 5.2 Showing the dimensions of the impellers

The rotation was controlled by a variable speed electric motor capable of speeds up to 750 rpm. A pipe at the base of the tank allowed material to removed from the base of the tanks. A T-section allowed material to be removed for samples and to be pumped through the recycle loop. A valve on each leg of the T-section controlled these flows. Material from the inline mixer was returned via a dip pipe located just above the uppermost agitator. A second dip pipe ending by the central agitator allowed the silicone oil to be injected into the agitator zone for the most efficient dispersion (El-Hamouz et al 2009). The tank walls were transparent so it was possible to check that no air was being entrained. A sealed lid on the tank had holes drilled in to it to allow the dip pipe and agitator axle to enter the tank.

5.2.2. Pump

The peristaltic pump draws fluid from the tank and pumps it to the inline mixer. It was capable of flowrates of the order of 1 l min^{-1}. The piping through the pump was silicone tubing.

5.2.3. Inline Mixer

The inline mixer was a Silverson L4RT Laboratory Mixer. It was fitted with the Laboratory Inline mixing assembly. The stator was the Square Hole High Shear Screen. The rotor speed was infinitely variable between 0 ~9300 rpm. The operating manual describes the mixer as being suitable for emulsification.

5.2.4. Recycle loop

In order to test the predictions of this extended model it was necessary to vary the volume of the recycle loop. This was achieved by using several large sections of piping that could be added or removed from the recycle loop. For the smallest possible volume all the

connections were made using a rubber hose of internal diameter 5 mm. This gave a recycle loop volume of 0.1 l.

To increase the loop volume a long section of the same hose was added between the Silverson and the tank. The long section was coiled around a large bucket in such a way as to encourage air bubbles to rise with the direction of flow from the inline mixer to the tank. This ensured there were no trapped air bubbles in the loop which would reduce its effective volume. With this extra loop the total volume of the recycle loop increased to 1 l.

A recycle loop volume of 2 l was achieved by additionally inserting a section of plastic hose between the Silverson and the tank. The internal diameter of this hose was 20 mm.

The largest recycle loop volume created was 3 l. This required a second section of

20 mm plastic hose to be added between the inline mixer and the stirred tank.. The joining sections between all these pipes were 40 mm long with an internal diameter of 3 mm..

The Reynold's number in a pipe of diameter *a* is given by,

Equation 5.1

$$\mathrm{Re} = \frac{\rho u a}{\mu} = \frac{4\rho F}{\pi \mu a}$$

So for a flow rate of 1 l min-1 the values of *Re* for the 3,5 and 20 mm sections of pipe are 7000, 4000 and 1000 respectively. The critical value for the onset of turbulence in pipes is ~2000 (Holland and Bragg 2005). This shows that the there will be both turbulent and laminar flow in the recycle loop which is undesirable. However as shown in the modelling section it is possible to incorporate this in to the description so it should not undermine the result.

These pieces of equipment enable a laboratory scale system to be created that replicates the industrial practice modelled in the literature (Baker 1993). The extra sections of piping allow the recycle loop to be varied between 3%-46% of the total batch volume in order to test the predictions of the extended model presented in the current work.

5.3. Analytical techniques.

The aim of the experiments is to test a model that predicts the drop size in the stirred tank and also to try and gain some understanding of the particular inline mixer. In order to reach these aims the drop size distributions need to be measured and the so do the speed and power of the inline mixer.

5.3.1. Sizing the Emulsion Droplets

The samples of emulsion were analysed using a Malvern Mastersizer 2000. The dispersed phase droplets scatter the laser light (El-Hamouz 2007) and the resulting patterns are used to generate the drop size distribution. This is presented as a discrete volume distribution. The drops are classed by diameter in 100 geometrically spaced classes spanning 0.02 – 2000 μm. The volume fraction in each class is reported and values of d_{32} and d_{43} are calculated. Drop diameters corresponding to cumulative volume factions of 0.1, 0.5 and 0.9 are also given. The required inputs are the refractive indices for the two phases and the selection of a standard operating procedure (SOP). The relevant SOP is for spherical particles. Refractive indices for tap water, 1 % SLES solution and silicon oil were measured with a Bellingham and Stanley RFM 390 Refractometer. The values were 1.334, 1.335 and 1.405 respectively.

5.3.2. Monitoring the inline mixer

The rotational speed and torque of the Silverson were measured by a TorqSense ® RWT 310,320 Series Transducer. Two digital temperature probes measured the temperature at the inlet and outlet. These measurements were channelled through a Pico Technology PT-104, PT 100 converter and recorded on a personal computer.

5.4. Experimental method

5.4.1. Calibration of pump speed

It was desired to know whether factors such as the liquid height in the tank, the operation of the inline mixer or the recycle loop volume would affect the flowrate in the recycle loop. The flowrate is required as an input in to the theoretical model. To measure this the recycle loop was disconnected from the dip pip returning it to the tank. It was directed instead in to a measuring cylinder. The volume in the cylinder was measured as a function of time. From this relationship the flowrate was found.

5.4.2. Preparation of initial coarse emulsion

The theoretical modelling assumed no droplet breakup in the stirred tank. To achieve this ideal the emulsion must have reached equilibrium so that there is no more dispersion in the stirred tank. By testing the time taken to reach equilibrium it was possible to have more confidence that the assumption was valid. The first step in preparing an emulsion was to prepare the aqueous phase. The SLES is 70% by weight active ingredient so to make a 1% by weight solution 45/0.7 = 64.3 g of SLES was added to 4500 g of tap water. Both quantities were measured to ± 0.1 g. A spare benchtop mixer in the laboratory was used to blend them for 30 minutes. This solution was used to make 3.5 ± 0.05 l of emulsion at an

oil phase fraction of 1 vol. %. To do this 3.45l of aqueous phase was charged to the tank.. Then the agitators were started at the desired speed (300 or 500 rpm). A syringe was used to inject 35 ml of silicon oil through the dip pipe to the central impeller region. Once the oil was injected a stopwatch was started and samples were taken periodically to determine the change of drop size with time.

To prepare the emulsions for the other experiments the same procedure was repeated with some variations. The quantity of oil varied. For a 5% volume phase fraction 175 ml would be added. Also the initial charge of aqueous phase was reduced. After the oil was injected the tank was then topped up to 3.5 l with aqueous phase. This was added through the dip pipe to flush through all the oil. This was not done when determining the change of drop size with time because it made it harder to define the point t=0.

For the recycle loop experiments up to 6.5 l of emulsion were required. This was beyond the capacity of the tank. To make this quantity the tank and recycle loop were charged with SLES solution and the agitator started. A quantity of oil in proportion to the total volume was added to the tank (e.g.5% of 6.5 l = 0.325 l). Then the peristaltic pump was started but not the inline mixer. The recirculation eventually distributes the oil evenly throughout the tank and recycle loop.

5.4.3. Investigation of the tank mixing time.

The assumption in the model is that the tank is well mixed. This is true if the mixing time is much less than the residence time. The residence time is given by $V/F \approx 3.5$ minutes. For tanks with three impellers $Nt_{95} \approx 200$ (Jahoda and Machon 1994) so for N = 300 rpm then $t_{95} \approx 40$ s. This less than the residence time but not an order of magnitude less. In addition the specific gravity of the oil is 0.97 and the density difference might lengthen the true mixing time. To avoid any doubt that this might be the cause of any deviations from the model in the literature (Baker 1993) the mixing in the tank was tested. 3.5 l of a high oil phase fraction emulsion was made in the tank. The agitator speed was set to 300 rpm. The emulsion was then pumped out from the bottom of the tank. Fresh SLES solution was pumped in to the tank so the fluid level remained constant. Samples were taken every minute. These samples were left to cream overnight. The height of the cream layer and the total depth of fluid were measured for each sample. The ratio of height of the cream layer to total height will be proportional to the oil phase fraction of the emulsion. In a well mixed tank the phase fraction should decrease exponentially, the exponent being $-Ft/V$.

This can be compared to the observed result to check whether the tank is well mixed or not.

5.4.4. A test of the volume averaging technique.

If a mixture is made up of *i* components with volume fractions C_i then the volume average drop size of the mixture is given by,

Equation 5.2

$$d_{43} = \sum_i C_i d_{43}(i)$$

Where $d_{43}(i)$ is the volume average drop size of component *i*. This is a crucially important result for the aim of this project. Measurements of $d_{43}(i)$ and calculations of C_i from the model will be used to predict d_{43} for comparison with the observations. It was therefore desired to quantify how accurately this could be done in practice. This required a situation where C_i was known. To do this an emulsion was used to accurately dispense measures of the emulsion in to samplw jars. The measures started at 50 ml and decreased in 5 ml steps to 0 ml. The remaining emulsion was then recycled through the inline mixer (operating at maximum speed) to reduce the drop size. This emulsion was then accurately pipetted in to the sample jars so that each contained a total of 50 ml of fluid. The Mastersizer was then used to measure the average drop size for each sample. If C_0 was the volume fraction of the first emulsion in the sample and C_1 the volume fraction of the second emulsion then the average drop size was,

Equation 5.3

$$d_{43} = C_0 d_{43}(0) + C_1 d_{43}(1)$$
$$d_{43} = d_{43}(1) + C_0 (d_{43}(0) - d_{43}(1))$$

So a plot of d_{43} against C_0 should yield a straight line.

5.4.5. Calibration of the sensors on the inline mixer

The TorqSense manual states that the speed and torque measurements are given as a voltage reading between 0 and 2.5 V. This relates linearly to speeds of 0-20,000 rpm and torque of 0-1 N m. The accuracy of the Picolog recorder was uncertain so it was tested. The rotational speed was independently measured with an optical tachometer. The speed of the Silverson mixer was varied. This was measured with the optical tachometer and the

voltage output from the picolog recorder was also recorded. The measurements were compared to assess the claim made in the manual.

These preliminary experiments were essential to check the basic assumptions in the model such as a well mixed tank where no drop breakup occurs. They also allow measurement of crucial parameters such as the recycle loop flowrate. The assessment of experimental accuracy will determine the confidence in the final conclusion.

5.5. Experimental tests of the theoretical model.

The first stage was to characterise the performance of the inline mixer. This data was combined with the calculated values of C_i to predict the change in d_{43} with time. Then the system was operated in recycle mode at different loop volumes. The drop size distribution at various times was measured and compared to the predictions of the model from the literature (Baker 1993) and the extended model developed in this work.

5.5.1. Characterising the inline mixer.

A coarse emulsion was prepared in the stirred tank as described above. A sample was taken to measure $d_{43}(0)$. The valves on the T-junction after the Silverson (see Figure 5.1) were adjusted so the emulsion would not return to the tank but be directed to a bucket for collection. The peristaltic pump and the inline mixer were then started and the whole batch passed through the mixer. A sample of this material was measured to determine $d_{43}(1)$. The emulsion was then pumped from the bucket back to the tank and the process repeated to determine $d_{43}(2)$, $d_{43}(3)$ etc. In repetitions of this experiment the material wa not pumped back in to the tank. It was pumped directly from the bucket, through the Silverson and in to another bucket. This was repeated back and forth. The buckets were manually atirred using a glass rod to ensure an even distribution in the buckets. This approach saved time: it was very quick to clean the buckets between passes but the stirred tank, with its sealed lid, took a lot longer. The outcome from this experiment was a series of values of $d_{43}(i)$ versus i that characterise the effect of repeated passes through the inline mixer.

5.5.2. Emulsification using an inline mixer in a recirculation loop of finite volume.

A laboratory scale version of an industrial emulsification technique was implemented. This is the procedure covered by the theoretical model. A coarse emulsion was prepared in the stirred tank as detailed above. At time t=0 the peristaltic pump and inline mixer were started. Material was pumped from the bottom of the tank, through the inline mixer and returned via a dip pipe to the top of the impeller region of the tank. Samples were withdrawn periodically from the bottom of the tank and measured using the Malvern

Mastersizer 2000. The result gave the volume average dropsize in the tank as a function of time. The model in the literature (Baker1993) and the extension developed here were used to predict the evolution of d_{43}. The models calculate C_i as a function of time. Combined with the values of $d_{43}(i)$ from the previous experiment d_{43} can be predicted by,

Equation 5.4

$$d_{43} = \sum_{i=0}^{\infty} C_i d_{43}(i)$$

Comparison between the models and the observations allowed the models to be evaluated. The experiment was repeated at different recycle loop volumes.

5.6. Summary

Suitable materials have been chosen to create emulsions for investigation. The preliminary experiments have been designed to check whether the equipment wa suitable and whether the proposed techniques were practical. The main experiments then directly addressed the aims of the project. Initially the secondary aim of characterising the mixer was addressed. The resulting information allowed the theoretical models to predict the change in d_{43} with time during the batch recirculation experiment. The comparison between the prediction and the measured values allows the model to be tested.

6. Experimental Results

Experiments have been conducted to first assess the capabilities of the equipment and then to address the aims of the research project. Tests measured the flowrate through the peristaltic pump and calibrated the electrical sensors. The mixing time in the stirred tank and the time taken to produce a coarse emulsion were determined by experiment. A mixture of known composition made from two emulsions was analysed. This demonstrated how accurately the volume fractions can be deduced from average drop size measurements. The effect of repeated passes through the inline mixer was determined. Finally a series of experiments produced batches of emulsion using the inline mixer in recycle loops of varying volume. The results were compared with the predictions of both the model in the literature (Baker 1993) and the proposed extension to include recycle loop volume.

6.1. Calibration of pump speed

Measurement of the flow rate in the recycle loop was conducted as described in the previous chapter. The peristaltic pump produces a flow which pulsates. It was observed that the degree of pulsation varied from day to day. Sometimes it would be very marked and at other times the flow would be almost perfectly smooth. This suggested that the flow rate might also be varying. The flow rates were measured for each experiment and were found to vary in the range 0.59 to 0.9 l min^{-1}. There was a strong effect of recycle loop volume, the longer loops leading to lower flowrates. But this was not the only factor. It was suggested that the mechanical action was pulling the tubing into the pumping zone and changing the volume that the rollers were acting on. Piping joins were placed at the entry and exit of the pump to stop the tubing being pulled through but this did not eliminate the variation. It appears that the silicone tubing inside the pump was stretching and changing the volume pumped per rotation. Once the silicone tubing split and when it was replaced the flow rate changed. This means that a constant value of the flowrate F could not be used. The flowrate is a crucial input for the models. Subsequently the flowrate had to be measured individually for each experiment.

6.2. Preparation of an initial, coarse emulsion

The progress of the production of a coarse emulsion was determined. The method has been described in the previous chapter. The evolution of drop size with time is shown below in Figure 6.1.

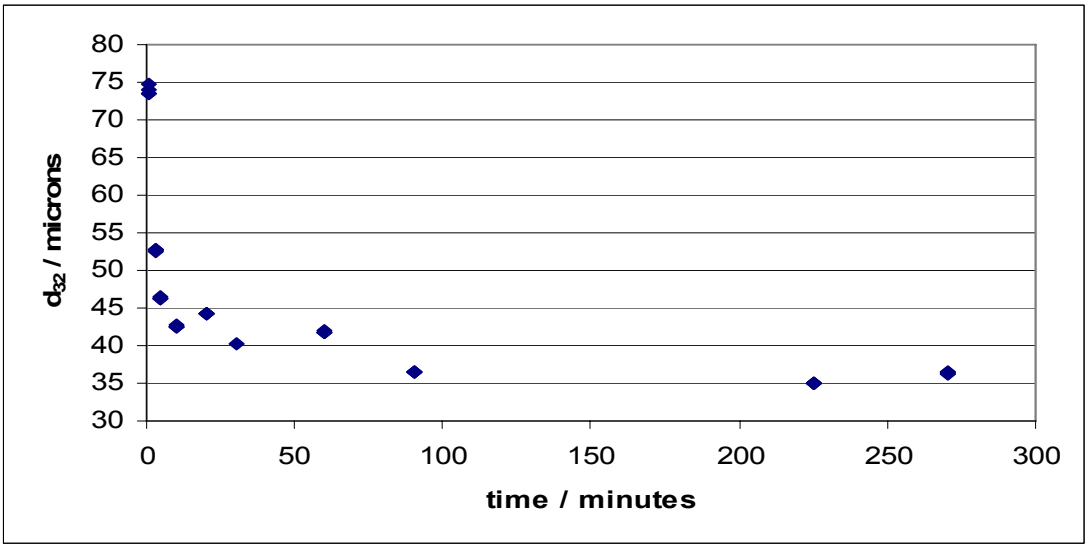

Figure 6.1 Showing the Sauter Mean Drop Diameter in the Stirred Tank Reducing With Time.

This emulsion was produced with the agitator speed set to 500 rpm. Figure 6.1 shows that the drop size decreases rapidly at first and then more slowly as time progresses. It strongly suggests that a stable equilibrium is reached after about 2 hours. This is in line with the results of other workers (Calabrese et al 1986). Other studies have been particularly concerned with accurately determining the equilibrium drop size to correlate against Weber number. Accordingly they have fitted their results with exponentially decaying functions and used the results to determine the point of equilibrium (El-Hamouz 2007). Precise determination of d_{32} is not the present aim. It is only sought to estimate a sufficient time beyond which no significant dispersion occurs in the stirred tank.

It was decided that operating the stirred tank at 500 rpm produced droplets that were too small. To improve the contrast with the inline mixer the agitator speed in the stirred tank was reduced to 300 rpm to prepare emulsions for the main experiments. A large variation in the size of the produced droplets was observed. The drop size seemed to depend on whether the emulsion was created with or without recycling in the loop (without operating the inline mixer). The batch drop size against the volume of recycle loop used for that batch is shown in Figure 6.2.

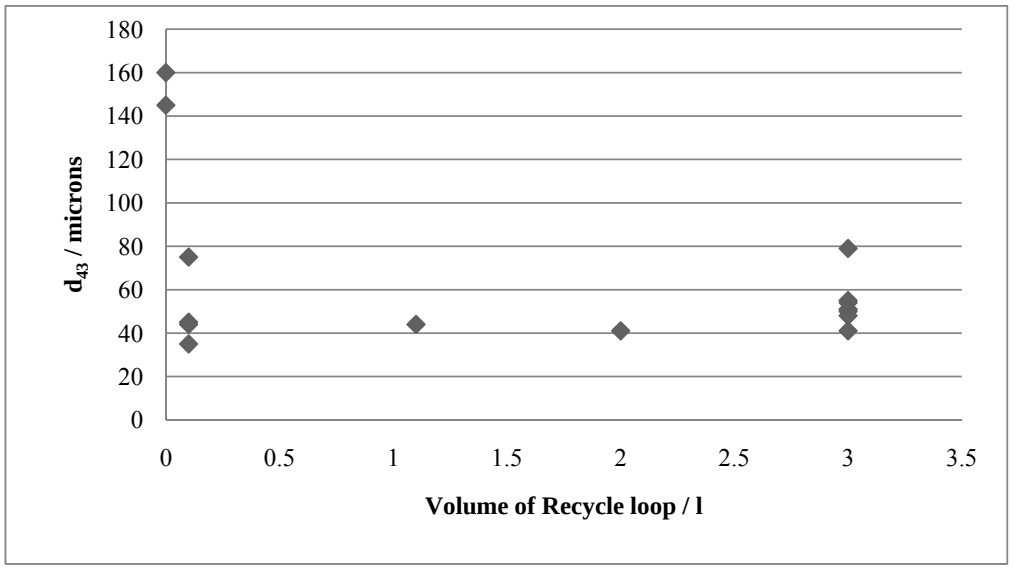

Figure 6.2 Showing the variation in drop sizes between batches.

Here a recycle loop volume of 0 refers to the case when the batch was not recycling through the loop. Figure 6.2 shows a marked reduction in the volume averaged drop size when the batch was created whilst recycling through the loop. Other observations were made that support the idea that this is caused by the trapping of large droplets in the pipes and not by the breakup of droplets in the pipe. The 20mm sections of pipe were semi-transparent and some droplets could be seen stuck to the pipe walls. When the recycle loop was being cleaned the tank and loop were flushed with fresh SLES solution. Even after more than 10 l had been flushed through it was noticed that occasionally a large globule of oil would appear in the effluent. A batch of 6.5 l was produced and the drop size in the tank was sampled. The recycle loop was drained in to a separate container and that drop size was sampled too. The values of d_{43} were 50 µm and 154 µm in the tank and recycle loop respectively. In the modelling section it was shown that distributive mixing throughout the system should only take around ten minutes so this confirms that the large drops must be stuck in the recycle loop.

These tests show that by preparing the batches overnight it was possible to ensure equilibrium had been reached. However they also show that the initial dropsize of the batches varied between ~40-80 µm. This large variation needed to be accounted for when characterising the performance of the inline mixer.

6.3. Investigation of the mixing time in the stirred tank

As explained in the previous chapter the quality of distributive mixing was investigated. Samples taken every minute were assessed to determine the reduction of the oil phase fraction in the tank. After being left overnight the samples had separated into two separate

layers; an opaque cream layer at the top and a clear layer at the bottom. The boundary between the two was sharp. The volume of the cream layer was determined as a fraction of the total sample volume and the results are shown in Figure 6.3.

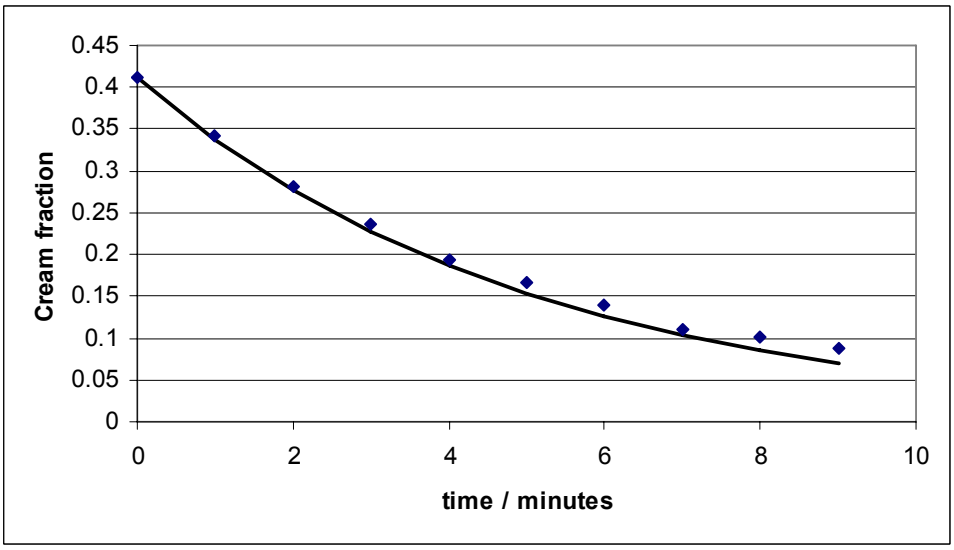

Figure 6.3 Showing the Volume Fraction of the Cream Layer Over Time

The points mark the experimental measurements. The flowrate was determined to be 0.69 l min^{-1} and the volume in the tank was 3.5 l. Consequently for a well mixed tank the cream fraction would be expected to be proportional to $e^{-Ft/V} = e^{-0.69t/3.5}$ with t measured in minutes. This prediction is plotted in Figure 6.3 as a solid black line. The agreement with the observations is very good and confirms that the tank can be considered well mixed. The height of the cream layer was measured to the bottom of the meniscus with an accuracy of ± 1 mm. The shallowest depth of the cream layer was 6 mm so the percentage error of ~17% would explain the deviations seen at 8 and 9 minutes.

6.4. Test of the volume averaging technique

Measurements of d_{43} were made for a mixture of a coarse and a fine emulsion. The volume fraction of the coarse emulsion was C_0. As explained in section 5.4.4 the results are expected to lie on a straight line. The solid line in Figure 6.4 shows the line of best fit. The correlation coefficient was 0.95. An earlier experiment produced a correlation of 0.92 and this improvement is probably a reflection of a developing technique.

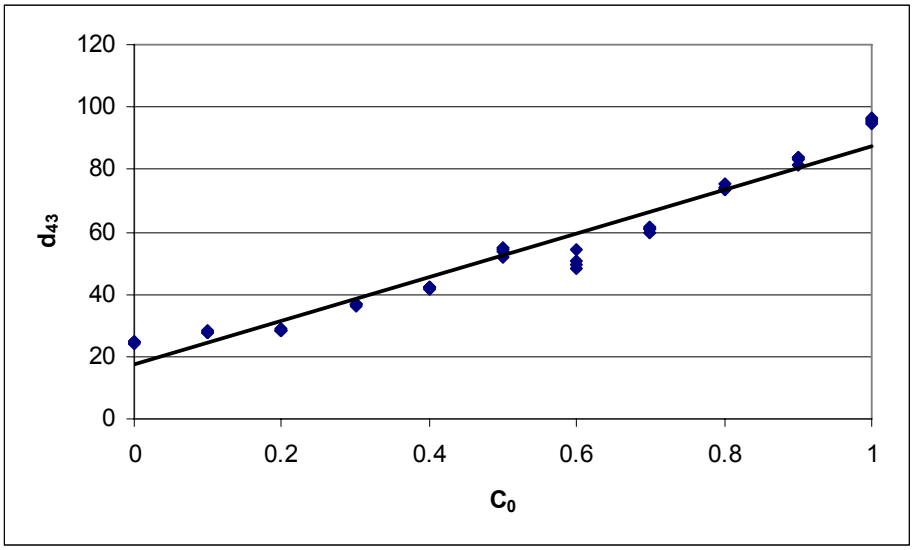

Figure 6.4 Showing d43 for another mixture of two emulsions

The point in Figure 6.4 corresponding to C_0=0.6 is worth noting. The Mastersizer takes three measurements of each sample over 30 s. These should be the same which is why most results look like a single point. The variation in d_{43} for this point is characteristic of a problem with the sample such as the entrainment of air bubbles. If this point is neglected then the correlation coefficient for the line of best fit increases to 0.97.

6.5. Calibration of the sensors on the inline mixer

The rotational speed of the inline mixer was independently measured with an optical tachometer and compared to the voltage output from the TorqSense transducer. These measurements confirmed the relationship claimed in the manufacturer's manual. It was not possible to make independent measurements of the torque. Since the rotational speed measurements were reliable it was assumed that the manufacturer's result for the torque measurements were similarly correct.

The temperature probes on the inlet and outlet of the mixer showed a negligible increase of $0.1\ ^\circ$C across the mixer. They also revealed that the background temperature varied from $22 - 29\ ^\circ$C.

6.6. Characterising the inline mixer

A batch of emulsion was repeatedly passed through the inline mixer to assess the effect on the average drop size. The inline mixer was operated at 5000 rpm. The first experiment showed an increase in the drop size after passing the mixture through the inline mixer. This was not expected. The change in the drop size distribution is shown in Figure 6.5.

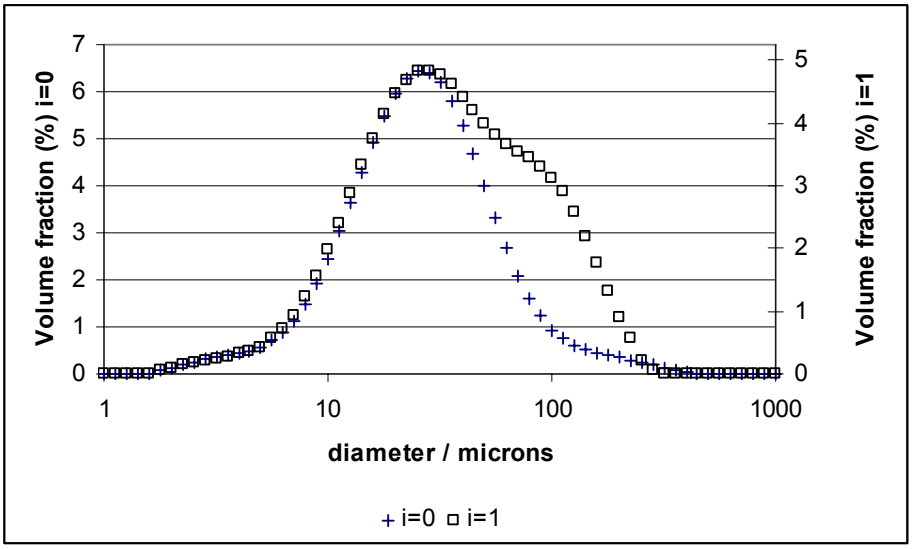

Figure 6.5 Showing the change in the drop size distribution after one pass through the inline mixer operating at 5000 rpm.

The distribution after passing through the mixer (i=1) is plotted on a secondary scale to show that the shape did not change at small diameters. This suggests that the increase in drop size is not due to coalescence of smaller drops to form larger drops. The observed change in Figure 6.5 would be consistent with the addition of larger drops. The suggestion is that when the emulsion was pumped back in to the stirred tank there was a residue of oil on the tank surfaces which contaminated the mixture. The experiment was repeated but the mixture was not pumped back in to the tank. Instead it was pumped from one bucket in to the next, which had been thoroughly cleaned. The results for two of these repeated experiments are shown in Figure 6.6. Fresh batches of emulsion were created for each emulsion which led to a difference in initial starting size as discussed above. It is not possible to discern a characteristic effect of the inline mixer from these results. For the initial size of 47 microns it is not clear that the mixer had any effect whatsoever on the emulsion. It was assumed that this was due to the mixer not being powerful enough.

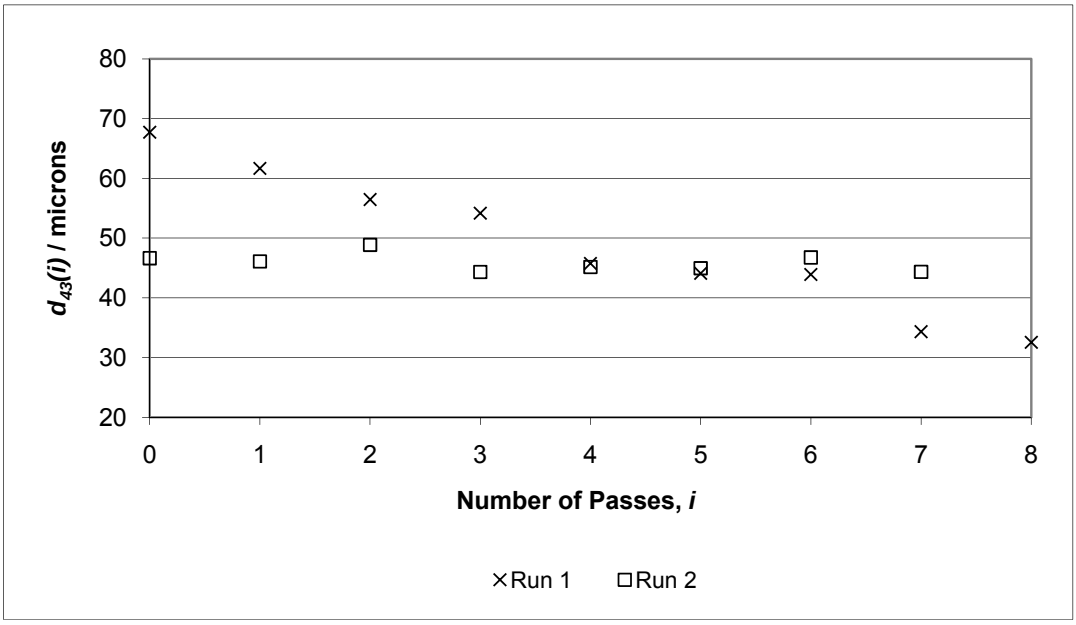

Figure 6.6 The effect of the inline mixer operating at 5000 rpm

The speed of the inline mixer was increased to the maximum 9300 rpm and the experiments were repeated several times. The results are shown in Figure 6.7.

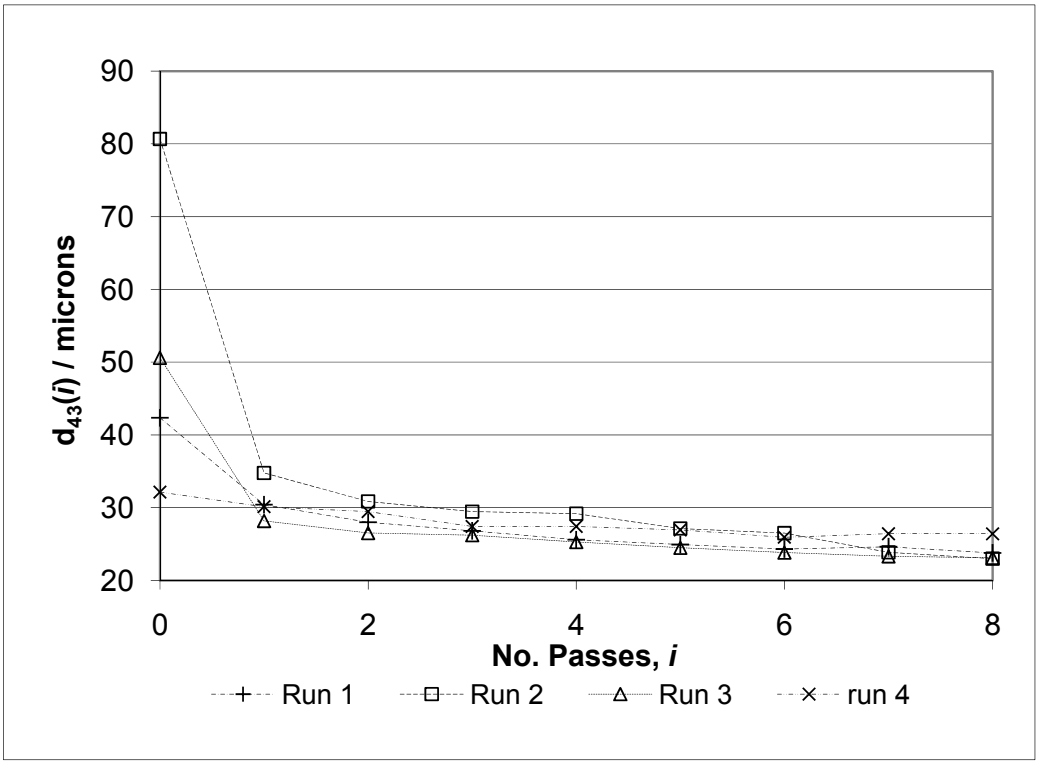

Figure 6.7 Showing the effect of the inline mixer operating at 9300 rpm

A fresh batch of emulsion was prepared for each experiment and led to a wide range of initial average drop size. Figure 6.7 shows that even when the initial drop size varies by ~50 μm the total range of variation is reduced to ~5 μm after just one pass through the inline mixer. In order to apply the numerical models to predict the drop size it is necessary to decide which values to use for $d_{43}(i)$. Figure 6.7 shows that if average values are used they will be correct to within ± 2 μm provided that the initial drop size falls within the range covered. The average values that have been used are shown in Table 6.1.

i	1	2	3	4	5	6	7	8
$d_{43}(i)$ / μm	31	29	27	27	26	25	25	24

Table 6.1 Showing the average values of $d_{43}(i)$

It is not necessary to use an average value for $d_{43}(0)$ since this can be directly measured for each case by taking a sample at t=0.

The change in the drop size distribution gives an idea of the effect of Silverson mixer. For the batch of initial drop size ~ 50 μm in Figure 6.7 the overall change in the drop size after 8 passes through the inline mixer is shown in Figure 6.8. The inline mixer was operating at the maximum speed of 9300 rpm.

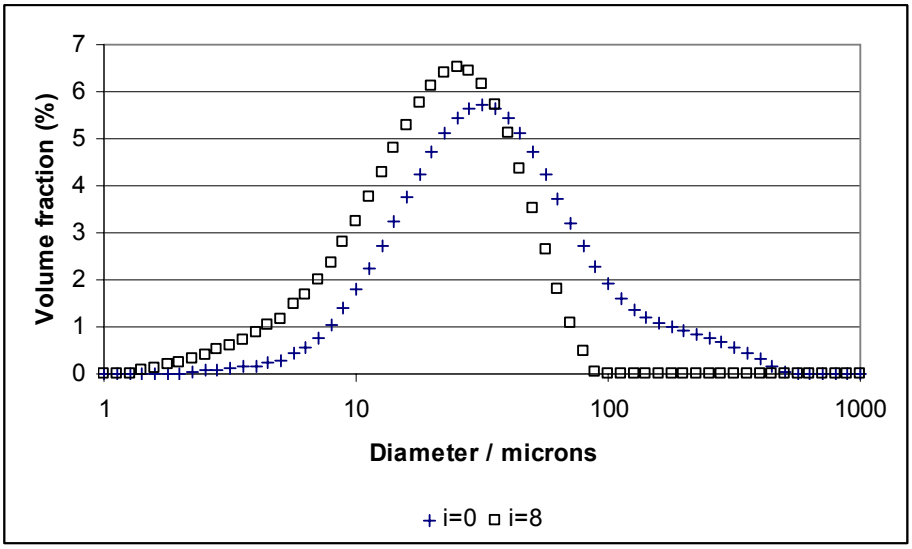

Figure 6.8 The change in drop size distribution after 8 passes through the inline mixer operating at 9300 rpm.

This shows that only the very largest drops were broken up and that there was not much change in the drop size distribution.

6.7. Emulsification using an inline mixer in a recirculation loop of finite volume.

The recirculation loop was operated at the smallest recycle loop volume of 0.1 l and the inline mixer speed was set to 9300 rpm. The values of V, ζ and F respectively were 3.5 l, 0.1 l and 0.9 l min^{-1}. The result is shown in Figure 6.9.

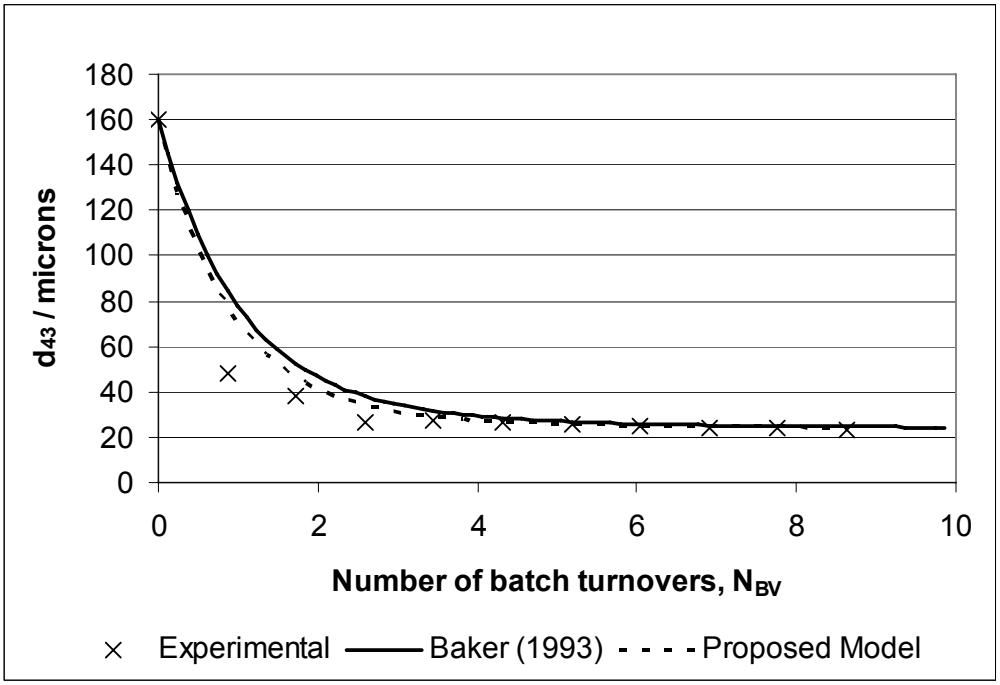

Figure 6.9 Drop size evolution for V =3.5 l, ζ =0.1 l and F =0.9 l min-1.

The solid and dashed lines in Figure 6.9 show the drop size predicted using the model of Baker (1993) and the extension developed here. The initial drop size was unusually large, even considering the variation experienced in these experiments. This means that the values of $d_{43}(i)$ in Table 6.1 might not be applicable. The experiment was repeated and the result is shown in Figure 6.10. For ζ =0.1 l the volume of the recycle loop is negligible so the model in the literature and the proposed extension produce very similar predictions. Both models give a very good fit to the observed data.

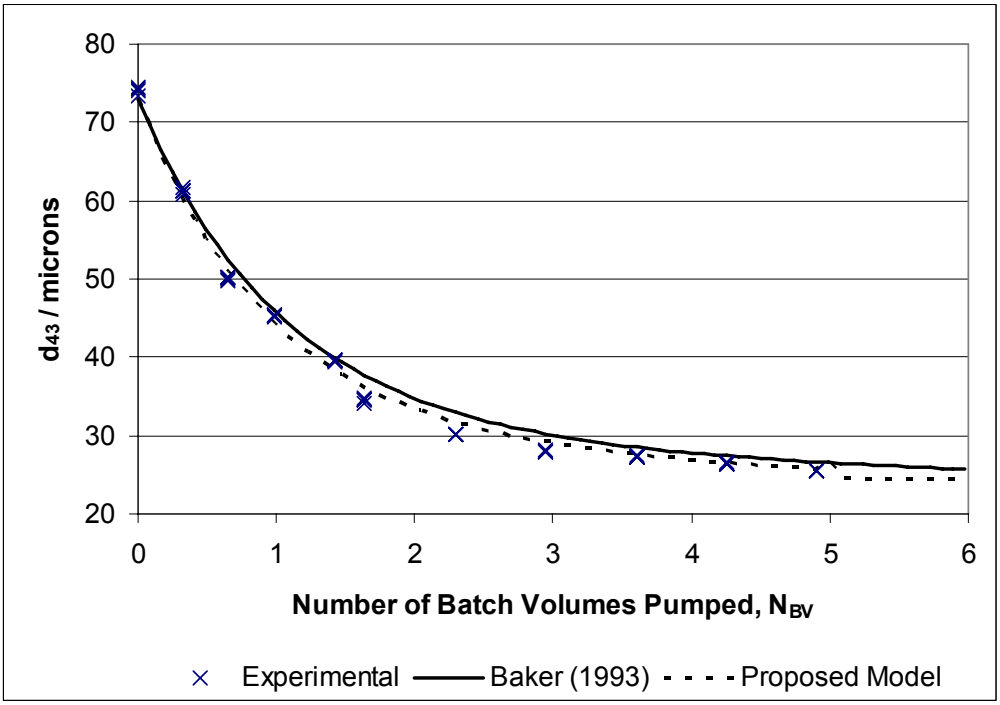

Figure 6.10 Drop size evolution for V=3.5 l, ζ =0.1 l and F =0.59 l min-1.

The recycle loop volume was increased to 1.1 l and the experiment was repeated. The flow in this loop was turbulent so the assumption of plug flow was used in the calculations of the proposed model. The results in Figure 6.11 show an initial period where the decline in drop size is delayed followed by a period of sharper decline than predicted by Baker (1993). These features are characteristic of the proposed model to incorporate the recycle loop volume.

Then the recycle loop volume was increased to 2 l and the experiment repeated. The flow in the first litre of the recycle loop was laminar, the flow in the second litre of the loop was turbulent. The proposed model used the description of a laminar section in series with a turbulent section to predict the results. The results are shown in Figure 6.12.

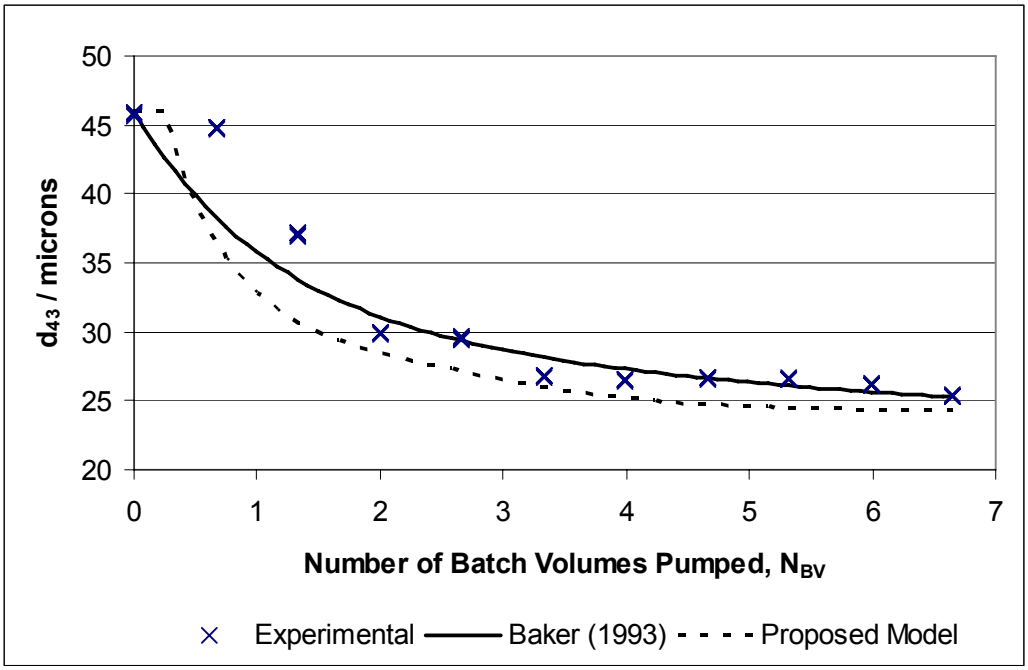

Figure 6.11 Drop size evolution for *V*=3.0 l, ζ =1.1 l and F =0.68 l min-1

The final drop size in Figure 6.12 is smaller than any produced when the mixer was being characterised. For this case the values for $d_{43}(i)$ are too large. This explains why the observed drop size declines more rapidly than predicted by either model.

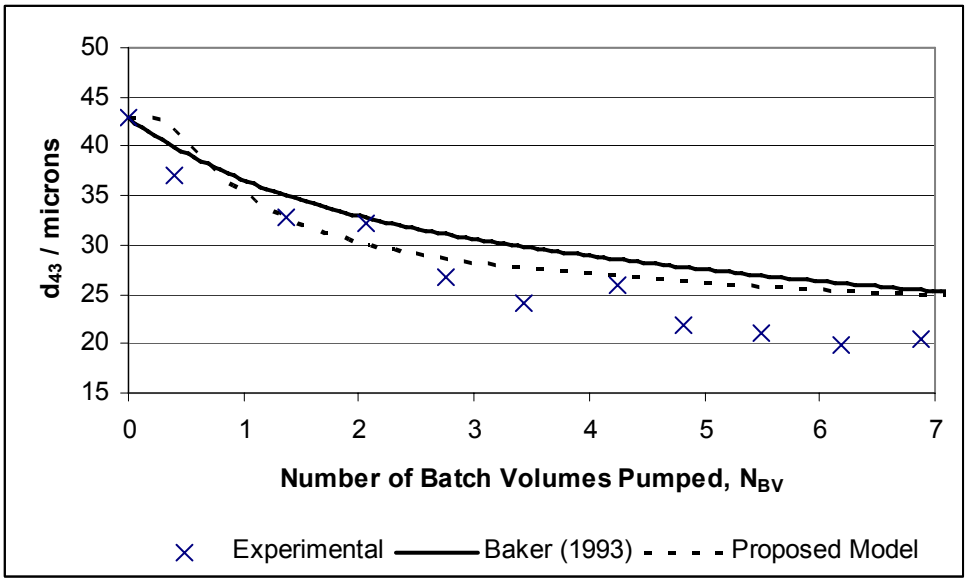

Figure 6.12 Drop size evolution for *V*=3.5 l, ζ =2 l and F =0.63 l min-1

Both Figure 6.11 and Figure 6.12 show that the differences between the two models are more pronounced at early times. They also show a need to repeat the experiments to clarify the degree of experimental variation. A decision was made to use the available time to focus on the effect at the largest recycle loop volume. The difference between the two models will be most clear for this case. Also more measurements were taken at early times to help clarify the difference between the two predictions. When the recycle loop was increased to 3 l the volume of the turbulent section was 1 l and the laminar section was 2 l. This was incorporated in to the proposed model. The experiment was performed three times and the results are shown in Figure 6.13, Figure 6.14, and Figure 6.15.

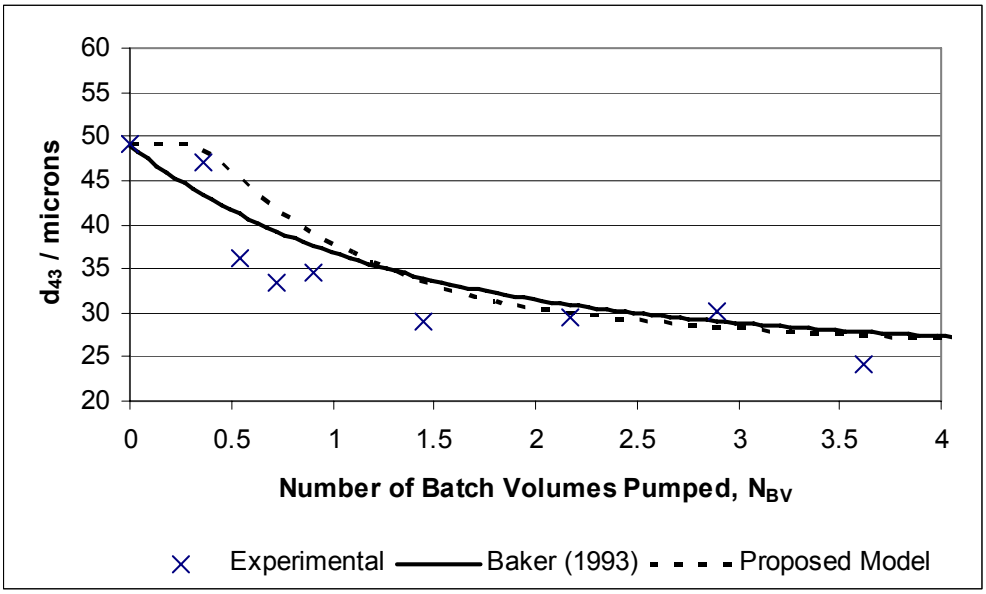

Figure 6.13 Drop size evolution for V=3.5 l, ζ =3 l and F =0.591 l min-1

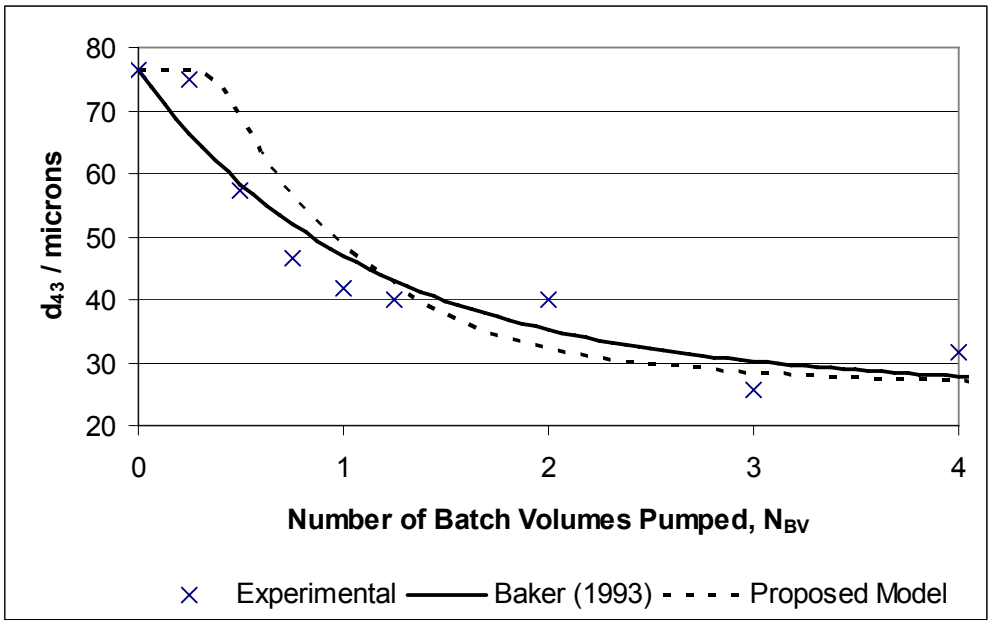

Figure 6.14 Drop size evolution for V=3.5 l, ζ =3 l and F =0.812 l min-1

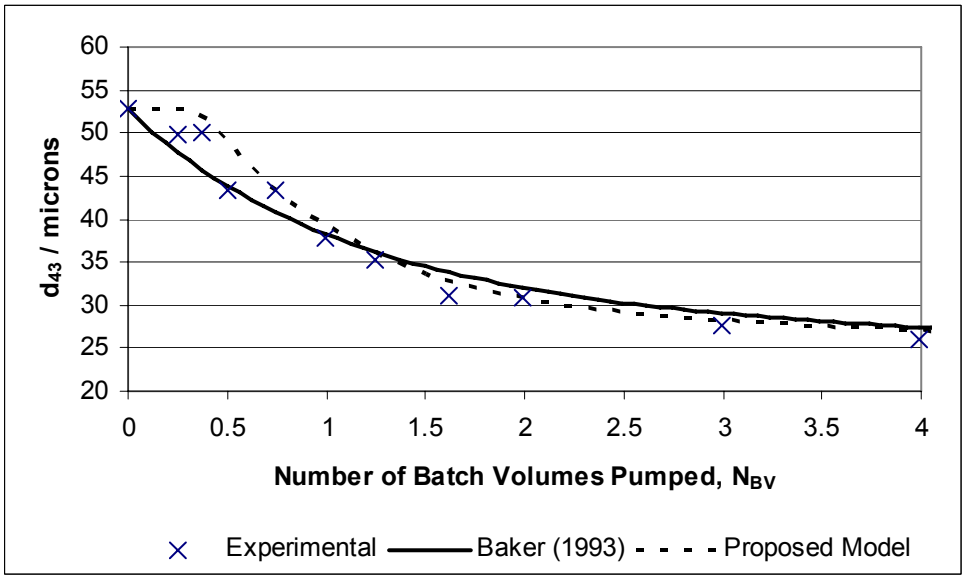

Figure 6.15 Drop size evolution for V=3.5 l, ζ =3 l and F =0.810 1 l min-1

For all these results both the model from the literature and the proposed extension are a reasonable fit for the experimental data. Particularly in Figure 6.14 and Figure 6.13 (also somewhat in Figure 6.15) it is possible to discern an initial period where the decline in drop size is slower than predicted by Baker (1993). This is followed by a period where the drop size declines more quickly than predicted by Baker (1993). These are the

characteristic features of the proposed extension to model the volume of the recycle loop. However the degree of scatter is similar to the predicted difference in drop size between the two models. This means it is not possible to conclusively state that the proposed model is significantly better just on the basis of a visual inspection of the results.

6.8. Summary

The tests showed that the electronic sensors were correctly calibrated. The flowrate in the recycle loop varied between 0.59-0.9 l min^{-1} and needed to be measured for each experiment. It took around two hours to produce an emulsion which is stable against further dispersion in the stirred tank. Before each experiment the batch was prepared for a much longer period overnight. Therefore the assumption that there is no breakup in the tank while the inline mixer is operating will be valid. However this method of production led to a wide range of initial drop sizes. The characterisation of the inline mixer addressed this point. Over a wide range of initial starting sizes the volume averaged droplet size after i passes was well determined to within $\pm$ 2 μm. These averaged drop sizes were determined for the first 8 passes. It was further shown that the Silverson was not much more effective than the stirred tank at dispersing the oil. This meant that useful measurements could only be made with the inline mixer operating at full power. Laboratory scale emulsification using an inline mixer in a batch recirculation loop was successfully performed for a range of recycle loop volumes. At the smallest volume the model of Baker (1993) and the proposed extension both led to excellent predictions compared to the observed progress of dispersion. As the recycle loop was increased the differences between the predictions of the two models also increased. It was possible to observe features characteristic of the proposed extension to the Baker (1993) model. There was an initial period of delay followed by a period when the drop size declined more rapidly than predicted by Baker (1993). However the difference between the two models was of a similar order to the degree of scatter in the results. This means it is not possible to conclusively prove that the proposed extension is more appropriate than the existing model.

7. Discussion

The experimental results demonstrate the effect of the recycle loop volume. They also allow some progress to be made towards characterising the inline mixer. These are two distinct problems and for clarity they should be considered separately. Firstly the issues with the performance of the equipment will be discussed in relation to the limits they impose on the accuracy achieved. This will compared to the results in the original investigation (Baker 1993). This enables some quantification to be made of the correlation between the model predictions and the experimental results.

The drop size distribution in the stirred tank suggests that this emulsion differs from those studied in the literature. This means that a standard population balance approach may not be suitable to characterise the mixer. Instead the effect of the mixer has been described as a matrix transformation. This sheds light on both the breakage function and daughter droplet distribution and will be useful for further studies on these devices.

7.1. The variation in initial drop size

The variation in drop size between batches suggests there was a lack of control and this might distract attention from the end result. However it is important to note that just recognising this variation represents an improvement on the approach taken by Baker (1993). The variability covers two issues. Firstly the effect of the recycle loop in drastically reducing drop size and secondly the more modest variation between batches made with the recycle loop. The causes of both can be identified but more importantly the characterisation of the inline mixer takes this variation in to account. This means that the primary aim is not compromised by these effects.

Figure 6.2 shows a large change in drop size from ~150 μm for batches made in the tank alone down to ~50 μm when the batches were recirculated while they were being made. This demonstrates that there is an effect on the average drop size due to passing through the loop which is separate from the action of the inline mixer. The models assume there is no such effect. In practice this assumption will still be valid provided that the effect has reached equilibrium before the inline mixer is started. This seems reasonable given that the batches were prepared for more than 12 hours overnight. The test of this assumption is in the results such as Figure 6.10. The goodness of fit shows that the effect does not impede the principal aim of modelling the distribution of C_i in the stirred tank. For this part of the investigation the absolute drop size is not important. It is necessary only that the drop size $d_{43}(i)$ can be correlated to the number of passes through the mixer, i.

Determining the dependence of $d_{43}(i)$ on fundamental parameters is a separate issue and is ruled out by the presence of an unknown factor. As a consequence this equipment is unsuitable for fundamental investigations in to the dispersion process: the observed drop size depends not only on the conditions in the tank or inline mixer but on some unknown process in the pipes. This is one factor that meant it was not possible to fundamentally characterise the Silverson mixer in the way that the literature characterises stirred tanks. Therefore for future work it would be helpful to eliminate this effect. It could be that at low flowrates the long sections of pipe approximate a settling tank where the cream rises and is trapped in dead zones in the pipe. However if this were the case the effect should not be seen for turbulent flow. Figure 6.2 shows that the effect is observed even when the loop volume is only 0.1 l. In this case the pipe diameter is 5 mm and the flow is turbulent. Silicon oils are known for sticking to surfaces and it seems likely that the larger drops are sticking to the equipment. Arai et al (1977) had a similar problem with a different oil and overcame it by adding polyvinyl chloride to the aqueous phase. This could alleviate the problem for future experiments.

Figure 6.2 shows that the majority of batches produced with the recycle loop were between 40-60 μm. In Baker (1993) his Figures 3 and 4 clearly show a variation in initial drop size between 38-55 μm. Despite this the predictions of his model all start from 50 μm at t=0. The actual range of $d_{43}(0)$ in Baker (1993) is ~ 17 μm. So the variation experienced in this work was not much worse than the results from the literature. Nevertheless it was desired to try and understand it by considering possible causes. From the Weber number correlation a variation in impeller speed would produce a variation in droplet size. This gives that $\frac{\Delta d_{32}}{d_{32}} = \left(\frac{\Delta N}{N}\right)^{-1.2}$. The speed setting on the electric motor was found to be inaccurate and measurements were made with an optical tachometer instead. This was accurate to within 3% which would only account for 1-2 μm of the observed variation in dropsize.

There is also an uncertainty in the phase fraction. The volume of oil was measured to within 0.5 ml and the volume in the tank to within 50 ml. So the typical volume fraction of the oil was 0.05 ± 0.001. The dependence of drop size on phase fraction varied between studies. But even using the relatively strong effect found by Mlynek and Resnick (1972) that $d_{32} \propto (1 + 5.4\phi)$ then this variance would barely account for 1 μm of the variation in d_{43}. The main source of the variation is likely to be the changes in temperature. El-Hamouz (2007) found ~30% reduction in drop size when the temperature increased from

$25 - 40\ ^{\circ}\mathrm{C}$ for the same oil and surfactant as used here. The range of temperature here is less but the temperatures are slightly lower and El-Hamouz (2007) showed that temperature changes produce greater effect at lower temperatures. So if a 15% in drop size due to the temperature changes is assumed then between this and the uncertainties in ϕ and N essentially all the variation of $50 \pm 10\,\mu\mathrm{m}$ in the drop size can be accounted for.

So the difference between this work and the previous study (Baker 1993) is not that there was variation in the initial drop size but that in this study it was accounted for. Figure 6.7 shows that whatever the initial value the drop size after passing through the inline mixer is very close to an average value. The range of initial sizes of 32-80 μm in Figure 6.7 covers all bar one of the batch emulsification experiments. This is a very important result since it shows that while the variation in initial drop size is not aesthetically pleasing it does not impede the determination of $d_{43}(i)$. This means it does not affect the ability to compare the theoretical models with the experimental results.

7.2. Stability of the recycle loop flowrate

Since the flowrate changed from day to day it is reasonable to question whether it remained constant during a given experiment. A typical batch emulsification using the inline mixer lasted 1 hour. Measurements of the flowrate only showed that it was constant over a period of three minutes. There was no way around this uncertainty. The flowrate could not be measured before a run since the measurement led to some foaming which could interfere with the measurements. It was assumed that the flowrate measured at the end applied to the whole process. If this was not the case then it would adversely affect the ability to compare the models with the experiment. It is not possible to prove that this was correct but the good correlation between the experiments and predictions strongly suggest that this was not an issue.

7.3. Validity of the volume averaging technique

The results given in Figure 6.4 are very important for estimating the practical limits of accuracy with which the theoretical models can be tested. Baker (1993) did not perform these checks but in this work they have been included to address any doubts about experimental competence. In these two tests the distribution (C_0 and C_1) is known precisely. The only error is in the measurements of d_{43}. The correlation with the lines of best fit gives a measure of the best possible agreement that could be achieved if the predictions of the model are exactly right. The predictions of the models also use values of $d_{43}(i)$ that are correct to ± 2 μm which introduces a further error. The lines of best fit in

Figure 6.4 gave correlation coefficients of R^2=0.92 and 0.95 respectively. This gives an objective measure of comparison to apply to the theoretical models.

7.4. Assessing the theoretical models

Both the models accurately predict the evolution of droplet size in the stirred tank. Within the degree of accuracy of this experiment it is not possible to definitively prove which one is better. This is more a consequence of the weakness of the inline mixer rather than a lack of any effect from the recycle loop volume.

Figure 6.10 reproduces the result of Baker (1993). The quality of the fit is just as good as achieved in that paper. Baker (1993) compared two inline mixers and his data for the orifice plate actually show a larger degree of scatter than observed in Figure 6.10. This result shows that the proposed model correctly reduces to the model used by Baker (1993) when the loop volume is small. It is also a validation of the experimental technique. Figure 6.2 shows that even with the smallest loop volume the effect of the oil phase sticking to the pipes is present. The reproduction of an established result confirms that this effect does not stop the equipment recreating the system envisioned by the models.

This also confirms that sufficient measurements were made for $d_{43}(i)$. Figure 6.7 shows that drop size was determined for up to eight passes through the mixer. Baker (1993) found this data for up to five passes through the first mixer and up to ten passes through the second. It might be argued that the drop size hasn't reached a minimum after 8 passes. However this is also true of the data in Baker (1993). The rate of decline at this point is so slow that it is reasonable to apply the value of $d_{43}(8)$ to material that has experienced more than eight passes through the mixer.

The results at intermediate recycle loop volume only show that both models fit the trend of the data. The difference in predicted drop size is too small compared to the scatter to distinguish between the two models.

The series of experiments at the largest recycle loop volume of 3 l give the best evidence in favour of the proposed model. In each of Figure 6.13, Figure 6.14 and Figure 6.15 there is a period of delay before the drop size starts to reduce. It is clear that the degree of scatter is similar to the difference between the models so the goodness of fit for each model was quantified. The correlation coefficient R^2 was calculated for the predictions of Baker (1993) and the proposed model. The values for Figure 6.13 were 0.81 and 0.79 respectively. The values for Figure 6.14 were 0.95 and 0.93 and the values for Figure 6.15 were 0.96 and 0.97. The general trend is that these values increase in the order in which

the experiments were performed. This probably reflects a growing consistency in using the Mastersizer to make the measurements. In Figure 6.13 the models were a relatively poor fit. This is probably just due to poor technique. The later experiments of Figure 6.14 and Figure 6.15 produced R^2 values that were comparable to those from Figure 6.4. This means that both models correctly predict the distributions of C_i to within the level of accuracy of this experimental method.

This similarity between the two models does not undermine the value of the proposed model but represents a difficulty specific to this system. The models calculate values of C_i which are used to predict the drop size. For the Silverson mixer the values of $d_{43}(0)$ and $d_{43}(1)$ are not very different. This means that the average drop size is fairly insensitive to the values of C_0 and C_1. At the pilot and industrial scales this will not be the case. In Baker (1993) the inline mixer produced drop sizes of microns rather than the tens of microns created here. In these situations the proposed model would predict a measurable departure from the standard model of Baker (1993). The obvious solution is to use a more powerful mixer for future experiments. It would also help if the sticking of large drops to the pipe walls could be eliminated. Figure 6.2 shows that this would lead to an initial drop size of ~150 μm and create a greater contrast between material that has and has not passed through the recycle loop.

7.5. Characterising the Inline Mixer

Before characterising the inline mixer it is interesting to characterise the stirred tank and compare this to the literature. This shows that standard relationships do not seem to apply. These standard relationships are used to justify the assumption of self-similar droplet breakup to solve the population balance equations. Therefore there is a need to try a different approach to modelling the droplet breakup in the inline mixer.

The stirred tank produced a very broad drop size distribution. The ratio of maximum drop size to minimum drop size was approximately 80. This is typical of non-coalescing systems. However the value of $d_{32}/d_{\max}$ was found to be approximately 0.14. This is significantly lower than the value of 0.6 typically found in the literature (Calabrese et al 1986a). This low value shows that the volume distribution cannot be described as Normal. Figure 6.8 shows that the initial drop size distribution is characterised by long tails at high and low drop diameters. There are few studies using the combination of high viscosity oil with surfactant to compare with. El Hamouz (2007) used the same oil and surfactant and his distributions show the same tail at small drop sizes. However he does not calculate or

comment on the value of $d_{32}/d_{\max}$. It seems likely that the reduced surface tension leads to a much greater stripping of small drops from the parent than has been observed without surfactant. Such a great quantity of small drops then leads to a much lower value of $d_{32}/d_{\max}$ than has previously been recorded.

The size of these small droplets ought to be determined more by the interfacial tension than the size of the parent droplet. For example the Kelvin-Helmholtz instability produces ripples at the interface between two fluids in relative motion which could lead to daughter droplets being stripped from the surface. The wavelength of these ripples is determined by the surface tension among other things. The size of the daughter droplets would be related to the size of the ripples. Provided these were much smaller than the parent drop diameter then the daughter droplets would remain the same size as the parent drop shrank. This is important in relation to the assumptions of self-similarity used to solve population balances. These methods assume that the size of daughter droplet relative to the parent is constant. A common test for similarity (Ramkrishna 2000 p205) has been applied to the data from Figure 6.1. The droplet diameter corresponding to a fixed cumulative volume fraction is plotted against time on logarithmic scales. Cumulative volume fractions of 0.1, 0.5 and 0.9 have been used as the data sets.

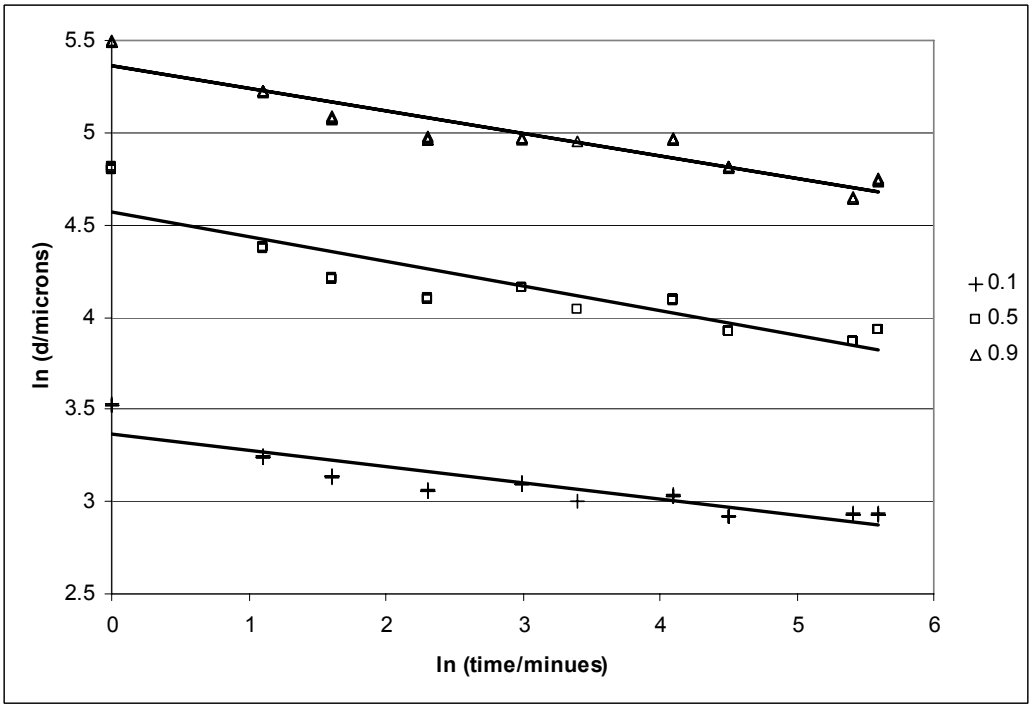

Figure 7.1 Similarity test for dispersion in the stirred tank.

If self similar behaviour was present then each set of data should produce a straight line and all the lines should be parallel. Figure 7.1 shows that the lines of best fit differ in gradient by over 30%. It is significant that the cumulative fraction of 0.1 does not fit with the other two. This is evidence to further support the analysis that the emulsion studied here leads to a much greater production of small drops than other studies in the literature and that consequently the standard methods of population balances will not apply.

Instead the effect of the inline mixer has been modelled as a matrix transformation acting on a vector representing the initial drop size distribution. The data from Figure 6.7 provide 32 vector equations to solve for the matrix. This was done according to the procedure detailed in the modelling section. The best fit solution for the matrix is shown in

	2.52	3.17	3.99	5.00	6.33	7.96	10.02	12.62	15.89	20.00	25.18	31.70	39.91	50.24	63.25	79.62	100.24	632.46
2.52	1.00	0.01	0.02	0.04	0.00	0	0	0	0	0	0	0	0	0	0	0	0.02	0.01
3.17		0.99	0	0.03	0.03	0	0	0	0	0	0	0	0	0	0	0	0.01	0.01
3.99			0.98	0.02	0.03	0	0	0	0	0	0	0	0	0	0	0	0.02	0.03
5.00				0.91	0.03	0.02	0	0	0	0	0	0	0	0	0	0	0.03	0.04
6.33					0.91	0.02	0.01	0.01	0	0	0	0	0	0	0	0.01	0.03	0.05
7.96						0.96	0	0	0	0	0.01	0.01	0	0	0	0.01	0.04	0.06
10.02							0.98	0	0	0	0	0.01	0	0	0	0.01	0.04	0.06
12.62								0.98	0	0	0	0.01	0.01	0	0	0.02	0.05	0.07
15.89									0.99	0	0	0	0.01	0.01	0.01	0.03	0.05	0.08
20.00										0.98	0	0	0.01	0.01	0.01	0.04	0.07	0.10
25.18											0.98	0	0	0.01	0.02	0.04	0.08	0.12
31.70												0.97	0	0.01	0.02	0.05	0.08	0.14
39.91													0.97	0	0.01	0.03	0.07	0.14
50.24														0.97	0	0.01	0.04	0.08
63.25															0.94	0	0	0
79.62																0.76	0	0
100.24																	0.37	0
632.46																		0.02

Figure 7.2 The breakage matrix characterising the effect of the Silverson Mixer operating at 9300 rpm

The headings for the columns give the upper size limit in microns of the class of the parent drop. The labels on the rows show the upper size limit of the class for the daughter droplets. Each column sums to one but the rounding means some values are not shown. This matrix very successfully calculates the dropsize distribution given a starting volume distribution and the number of passes through the mixer. An example is shown Figure 7.3.

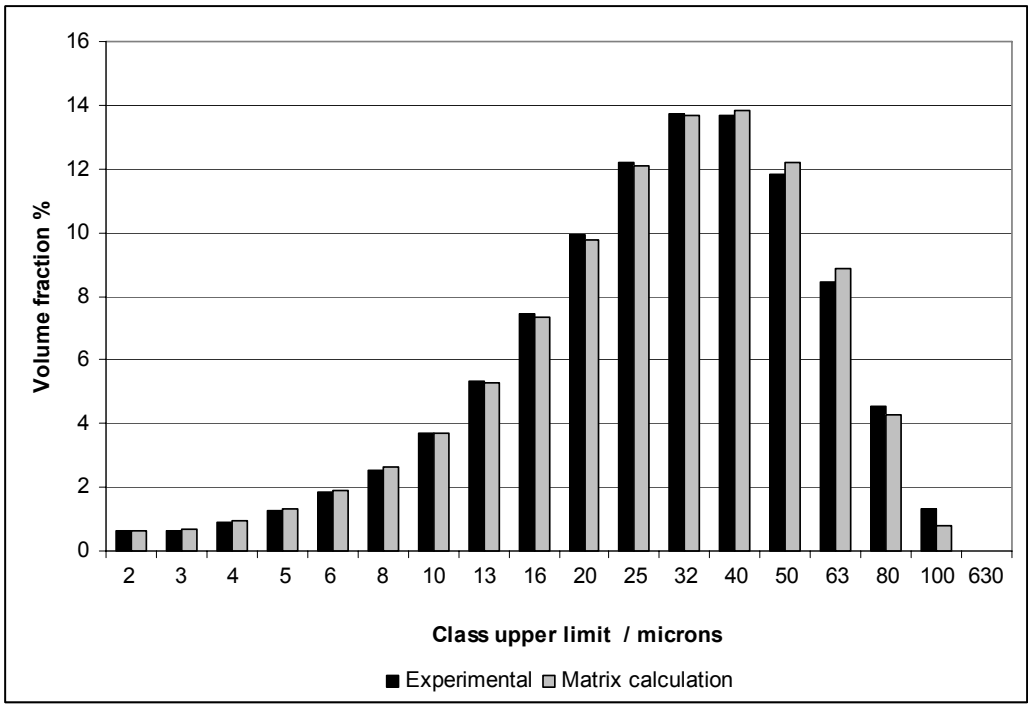

Figure 7.3 Predicted and observed drop size distributions after passing a batch twice through the inline mixer operating at 9300 rpm.

This matrix is a very powerful tool for gaining insight in to the function of the mixer. The column headed 100.24 shows the fate of drops classed with diameters between 79.62 and 100.24 μm. The entries of the column show the volume fraction that is transferred to the other classes. For instance the top entry shows that 2% of the volume in this class will be transferred to drops less than 2.52 μm across whereas the bottom entry shows that 37% of the volume remains in the original size category. This information is shown graphically in Figure 7.4.

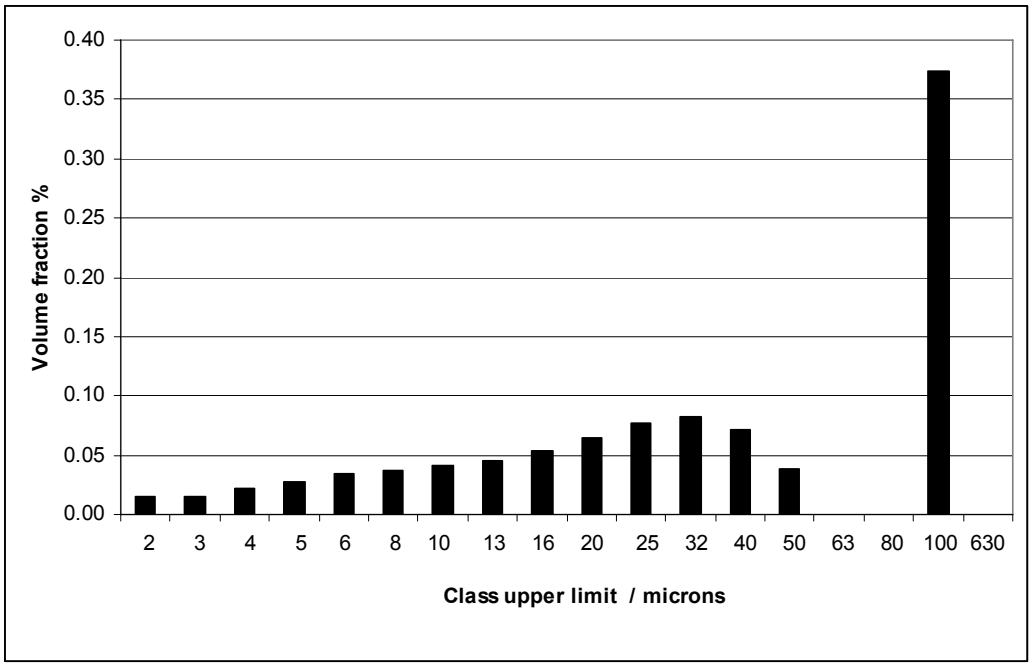

Figure 7.4 The daughter droplet distribution for parent droplets between 80-100 µm

This is a remarkably clear result giving a very good picture of the daughter droplet distribution. There seem to be no other studies in the literature that have achieved this without making a priori assumptions about the form of the daughter droplet distribution. This is often assumed to be either U-shaped or Normally distributed. Figure 7.4 shows that in the present case neither form is appropriate as the daughter droplet distribution is very broad with a long tail towards small drop sizes. Any attempt to apply the standard assumptions would have produced an incorrect result.

Figure 7.4 shows that only 37% of the initial volume survives in the 80-100 µm class. But when very small droplets are stripped from a large parent the volume of the parent doesn't change significantly. Consequently 63% would be an underestimate of the true breakage probability per pass.

There is no information in the literature about daughter droplet distributions produced by rotor stators. Nor is there any such data any viscous oils stabilised by surfactants so this result is a useful contribution. It also offers a way of objectively assessing rotor stators that could fill the current gap. If the breakage matrix for two devices was known then it would be possible to objectively compare their performance without physical experimentation. The elements of the matrix could be related to variables such as the rotor speed, the droplet viscosity and the surface tension. Then there would be an way to predict the performance of a rotor stator. If a change in supplier necessitated using a more viscous

oil in a product then the number of passes required for successful dispersion could be calculated and the impact on production rate estimated. The only criticism is that the numerical procedure for calculating the matrix has not been rigorously understood so the size of the errors cannot be quantified. Nevertheless comparison with experimentally observed distributions such as Figure 7.3 shows that the approach is valid.

7.6. Summary

The inconsistency in initial drop size and other factors relating to the equipment did not impede the experiments. The results of Baker (1993) were replicated for a negligible recycle loop volume. At larger loop volumes there is some evidence of the characteristic behaviour predicted by the proposed model. However the weakness of the effect of the inline mixer made it very difficult to distinguish between the proposed model and the existing model in the literature. Within the limits of experimental error both models were shown to be a good fit for the data.

A similarity analysis was applied to the breakup of droplets in the stirred tank. This showed that similarity does not apply for this system. This is believed to be due to the combination of viscous oil and surfactant leading to smaller daughter droplets. Since the standard methods of population balance modelling would not be appropriate in this case an alternative approach was employed. The effect of the mixer was characterised by an 18×18 matrix. This correctly matches the observed evolution of droplet size distribution after repeated passes through the mixer. The matrix reveals new information about the daughter droplet distribution and breakage functions. It offers an objective measure with which to compare mixers and predict their performance in dispersion applications.

8. Conclusions

8.1. The effect of recycle loop volume

A model has been developed to account for the effect of recycle loop volume. As the recycle loop volume tends to zero this model reproduces the solution of the existing model from the literature. The mathematical description made it possible to identify two key features that differentiate between the existing solutions and those that are predicted to apply when the recycle loop is large. Firstly the distribution of material in the stirred tank was shown to be narrower when the recycle loop was larger. Secondly the fraction of material in the tank that has not passed through the mixer remains constant for a short initial period. Then it declines at a faster rate than expected if the recycle loop volume is ignored. The result of this is that better results are likely to be achieved at laboratory scale than are possible at the industrial scale. In order to achieve similar results the number of batch volumes pumped will need to be increased at larger scales. The degree of increase was shown to depend on the change in recycle loop volume and the specification required. The effect is larger where the values of NBV are smaller. This means it will be more important for emulsification than for dispersion of solid powders which typically require hundreds of batch volumes to be pumped. An example calculation demonstrated that for a reasonable specification the NBV increased by nearly 14% on scale up to industrial scales. This will have a large impact on the economic evaluation and plant scheduling and therefore this effect needs to be taken in to account in process design.

8.2. Experimental validation of the model

An experimental method described in the literature was used to determine the distribution inside the stirred tank. This method was improved for the present investigation. Allowance was made for the time taken for the coarse emulsion in the stirred tank to reach equilibrium. Additionally the variation in initial drop size was recognised. The mean diameter after passing through the Silverson was shown to be only very weakly dependent on the initial drop size. Within the limits of the variation experienced it was possible to apply the approach taken in the literature. This eliminated two possible causes of deviation from the predictions of the established theory which would otherwise reduce the strength of the conclusions.

Two factors particular to the experimental set up might also lead to doubts about the conclusions but they have been addressed. Firstly the flow regime in the recycle loop varied between turbulent and laminar. There might be some ambiguity about the proper way to model this. However the theoretical calculations showed that both cases lead to

very similar distribution profiles. Therefore the precise details about the flow in the pipes will not make a material difference to the results. Secondly it was shown that passage through the pipework did reduce the drop size in the stirred tank, contrary to assumptions in the model. This effect was present even at the smallest recycle loop volumes. An excellent reproduction of the result from the literature was achieved at this volume. This showed that the effect must have reached equilibrium so the assumption of the model was correct. The maximum stable drop size in the stirred tank was very much greater than the smallest. This is typical of non-coalescing systems and validates the assumption to ignore coalescence. For these reasons it is possible to conclude that the experimental system accurately reflected the situation covered in the model.

The experimental observations showed evidence of the characteristic features of the proposed model. Within the limits of experimental accuracy it was shown that the proposed model was a good fit to the data. However within the same limits the original model from the literature was also a good fit. This reduces the strength of the conclusions that can drawn. The predictions of the proposed model were supported by the results. It was not possible to conclusively demonstrate that it gives an improvement over the existing model. This does not reduce the significance of the theoretical results. It is a consequence of using a relatively weak inline mixer. In industrial situations the effect of recycle loop still needs to be considered.

8.3. Characterising the dispersion

The drop size distribution of emulsions in the stirred tank was unusual in comparison with those described in the literature. The ratio of Sauter mean diameter to maximum rop diameter was very low. An analysis of the evolution of the drop size in the stirred tank showed that it did not follow the self-similar form that is often used to characterise breakage in stirred tanks. Consequently the standard approaches are likely to be unsuitable for characterising the rotor-stator. Instead the effect of the mixer was successfully characterised as an 18×18 matrix transformation. This level of detail requires 18 drop size distribution measurements to determine aa unique solution. 32 were used so a unique solution exists. The method of finding the matrix has not been fully understood. It has not been possible to quantify with confidence how close it is to the real solution or whether it represents a local minima in the sum of squared errors. However comparison between the predicted and observed distributions shows that the fit is very good. This confirms the validity of this new approach.

Because the accuracy of the matrix is unknown it is difficult to draw detailed conclusions from its structure. However some broad points can be made. The daughter droplet distribution is broad with a long tail towards smaller drop sizes. There appears to be a gap of about 2 classes between the parent and the largest daughter. This could indicate that a breakup event consists of a great number of daughter drops being shed at once. An interesting feature of the matrix is that it suggests that smaller parent drops do not produce the smallest daughter drops. Physically this could be explained by the increased Laplace pressure creating a more stable surface that resists the shortest wavelength disturbances. It is an interesting result since it contradicts the assumption of similarity whereby smaller parents produce smaller daughters. This level of analysis is too subtle given the lack of understanding about this new technique so these observations cannot be firm conclusions. What is clear is that the daughter droplet distribution is not well described by a Normal distribution or a U-shaped curve. Thus the common assumptions of population balance models are not appropriate for this case.

8.4. Recommendations for further work

It would be desirable to have definitive confirmation of the theroretical predictions about the effect of the recycle loop's volume. This could be achieved by repeating the experiments using a more powerful inline mixer. Changing the oil used, or adding chemicals to the aqueous phase could stop the oil phase sticking to the pipes. This would lead to larger initial drop sizes in the tank and further increase the contrast with the processed material. The results of the theoretical model could then be applied with confidence.

The proposed model predicts that emulsions could be produced more efficiently in a plug flow recycle loop than in a well mixed tank. It was suggested that a multi-stage mixing tank could provide a compromise between the desired plug flow and the necessary distributive blending. The potential savings in production time were up to 80%. The improved control over the drop size distribution could increase product value. Therefore it would be worthwhile to investigate the practicality of this suggestion.

The matrix characterisation of the inline mixer opens up many avenues for further research. The theoretical understanding behind it needs to be developed. Experimental errors mean that the matrix inversion is ill-posed. Techniques for regularising the data need to be applied to quantitatively assess the errors in determining the elements. With better techniques and more data the matrix could be determined to a more accurate resolution. A 55×55 matrix would be needed to fully capture the level of detail provided

by the Mastersizer measurements. Once this method is understood it could be applied to develop fundamental understanding of both the dispersion process and rotor-stators. Changes in viscosity, interfacial tension, rotor speed or stator design could all be related to their effect on the daughter droplet distributions and breakage function. Once characterised the performance of a mixer on new products could be predicted. Objective comparison between mixers could also be made. There is relatively little published work on the performance of rotor stators so this work would very productive.

There has been very little other work on emulsions of viscous oils stabilised by surfactant. The results here suggest that the sizes of the daughter droplets are not related to the size of the parent. This could mean that the proportional relationship between d_{32} and d_{max} does not apply. It would be worth investigating this relationship to see if it does apply in this case. The could be significant for process design. If the relationship does not hold then correlations with d_{32} will not hold either and d_{max} will need to be used instead.

The viscosity group identified by Hinze (1955) has been shown to only be relevant for small deformations (Sleicher 1962). The results here suggest that small deformations at the surface are creating small daughter drops. Therefore the viscosity group of Hinze might be more appropriate in this case. This would contrast with the studies in the literature which looked at oils without surfactant and correlated the viscous resistance using the viscosity group of (Calabrese et al 1986a). By varying the viscosity of the oil phase this could be tested.

Nomenclature

Symbol	Description	Dimensions	Units
a	Pipe diameter	L	mm
b	width of hole in stator	L	mm
B	Constant	-	-
B_V	Total Batch volume	L^3	l
C_i	Fraction of material in the stirred tank that has passed through the mixer i times	-	-
C'_i	Fraction of material returning to the stirred tank that has passed through the mixer i times	-	-
d	drop diameter	L	µm
D	Impeller diameter	L	cm
d_{32}	Sauter mean diameter	L	µm
d_{43}	Volume averaged drop diameter	L	µm
$d_{43}(i)$	Mean diameter after i passes through the mixer	L	µm
$D_{brownian}$	Brownian motion diffusion coefficient	$L^2\ T^{-1}$	$m^2\ s^{-1}$
d_j	Midpoint diameter of the jth size class	L	µm
d_{max}	Maximum stable drop size	-	-
D_{mol}	Molecular diffusion coefficient	$L^2\ T^{-1}$	$m^2\ s^{-1}$
$D_{turbulent}$	Virtual diffusion coefficient	$L^2\ T^{-1}$	$m^2\ s^{-1}$
F	Flowrate	$L^3\ T^{-1}$	$l\ min^{-1}$
k	Wavenumber	L^{-1}	m^{-1}
L	Pipe Length	L	m
l	Eddy length	L	m
N	Agitator rotational speed	T^{-1}	rpm
N_{BV}	Number of batch volumes pumped	-	-
n_j	Number of particles in the jth size class	-	-
N_{Vi}	Viscosity group (Hinze 1955)	-	-
P	Power	$M\ L^2\ T^{-3}$	W
P_0	Power number	-	-
Re	Reynolds number	-	-
S	Mixing length	L	m
t	Time	T	minutes
t_{95}	Mixing time	T	s
T_{Kelvin}	Absolute Temperature	θ	K
u	fluid velocity	$L\ T^{-1}$	$m\ s^{-1}$
u_0	fluid velocity in centre of pipe	$L\ T^{-1}$	$m\ s^{-1}$
V	Stirred tank Volume	L^3	l
v^*	Wall Friction velocity	$L\ T^{-1}$	$m\ s^{-1}$
Vi	Viscosity group (Sleicer 1962)	-	-
Vi'	Viscosity group (Calabrese et al 1986a)	-	-

We	Weber number	-	-
We_{crit}	Critical Weber number	-	-
Z	Constant	-	-

Greek Symbols

δ_{gap}	gap between rotor and stator	L	mm
ε	Rate of energy dissipation	$L^2\ T^{-3}$	$W\ kg^{-1}$
ζ	Recycle loop volume	L^3	l
η	Kolmogorov scale length	L	µm
θ_j	Volume fraction of droplets in j^{th} size class	-	-
μ	Viscosity	$M\ L^{-1}\ T^{-1}$	Pa s
ν	Kinematic viscosity	$L^2\ T^{-1}$	St
ρ	density	$M\ L^{-3}$	$kg\ m^{-3}$
σ	Interfacial tension	$M\ T^{-2}$	$N\ m^{-1}$
$\sigma_{dynamic}$	Dynamic surface tension	$M\ T^{-2}$	$N\ m^{-1}$
τ	External shear stress	$M\ L^{-1}T^{-2}$	$N\ m^{-2}$
φ	Dispersed phase volume fraction	-	-

Functions

$E(k)$	Turbulent energy spectrum
$b(d)$	Breakage function
$P(d\|d')$	Daughter droplet distribution
$\nu(d)$	Number of daughter droplets

Constant

k_B	Boltzmann Constant	$1.381x10^{-23}\ kg\ m^2\ s^{-2}\ K^{-1}$

References

Ali, A.M., Yuan, H.H.S, Dickey, D.S. and Tatterson G.B. (1981) Liquid dispersion mechanisms in Agitated tanks. I: Pitched Blade Turbine. *Chem. Eng. Commun.* **10** 203

Alves, S.S., Vasconcelos, J.M.T. and Barata, J. (1997) Alternative compartment models of mixing in tall tanks agitated by multi-Rushto-Turbines. *Trans.I.Chem.E.* **75** Part A 334-338

Arai, K., Konno, M., Matunaga, Y. (1977) Effect of dispersed phase viscosity on the maximum stale drop size for breakup in turbulent flow. *Journal of Chem. Eng. of Japan* **10** 4 325-330

Baker, M.R. (1993) Droplet breakup using inline mixers located in recirculation loops around batch vessels. *Chem.Eng. Sci.* **48** 22 3829-3833

Baldyga and Bourne (1999). Turbulent Mixing and Chemical Reactions. UK; John Wiley & Sons Ltd, ISBN 047198171 0

Barailler, F., Heniche, M., Tanguy, P.A. (2006) CFD analysis of a rotor stator mixer with viscous fluids. Chem. Eng. Sci. 61 2888-2894

Becher, P. (2001) Emulsions: Theory and Practice New York; Oxford University Press. ISBN 0-8412-3-496-5

Bourne, J.R. and Studer, M. (1992) Fast reactions in rotor stator mixers of different size. *Chemical Engineering and Processing* **31** 285-296

Brocart, B., Tanguy, P.A., Magnin, C. and Bousquet, J. (2002) Design of inline emulsification processes for water-in-oil emulsions. *J. Dispersion Science and Technology*. **23** 45-53

Brown, D.E. and Pitt, K. (1972)Drop size distribution of stirred noncoalescing liquid-liquid systems. *Chem.Eng.Sci*. **27** 577-583

Calabrese, R.V., Chang, T.P.K. and Dang, P.T. (1986a) Drop breakup in turbulent stirred tank contactors. Part I Effect of dispersed phase viscosity. *A.I.Ch.E Journal* **32** 4 657-666

Calabrese, R.V., Wang, C.Y., and Bryner, N.P.(1986b) Drop breakup in turbulent stirred tank contactors. Part III Correlations for mean size and drop size distribution. *A.I.Ch.E. Journal* **32** 4 677-681

Chang, T. P. K., Sheu, Y. H. E., Tatterson, G. B. and Dickey, D. S.(1981)'LIQUID DISPERSION MECHANISMS INAGITATED TANKS: PART II. STRAIGHT BLADE AND DISC STYLE TURBINES',*Chem.Eng.Commun.,***10** 4 215 —222

Chen, H.T., and Middleman, S. (1967) Drop size distribution in agitated liquid-liquid systems. *A.I.Ch.E Journal* **13** 5 989-995

Cohen, D (2005) High shear mixing: don't fall victim to common misconceptions. Chemical Engineering April 2005 46-51

Cristini, V., Bladwzdziewicz, J., Loewenberg, M. and Collins, L.R. (2003) Breakup in

D'Aquino, R.(2004)Masterminding mixing technology. *Chemical Engineering Progress* **100** 8 7-10

Davies, J.T. (1987) A physical interpretation of drop sizes in homogenizers and agitated tanks, including the dispersion of viscous oils. *Chem.Eng.Sci.* **42** 7 1671-1676

Desnoyer, C, Masbernat, O., Gourdon, C. (2003) Experimental study of drop size distributions at high phase ratio in liquid liquid dispersions. *Chem. Eng. Sci.* **58** 1354-1363

El-Hamouz, A. (2007) Effect of surfactant concentration and operating temperature on the drop size distribution of silicon oil water dispersion. *Journal of Dispersion Science and Technology* **28** 797-804

El-Hamouz, A., Cooke, M., Kowalski, A. and Sharratt, P. (2009) Dispersion of silicone oil in water surfactant solution: effect of impeler speed, oil viscosity and addition point on drop size distibution. *Chemical Enginering and Processing* **48** 633-642

El-Jaby, U.,McKenna, T.F.L., Cunningham, M.F. (2007) Miniemulsification: an analysis of the use of rotor-stators as emulsification devices. *Macromol. Symp. 2007* 259 1-7

Etchels, A.W. and Meyer, C.F. (2004). Mixing in pipelines. In Handbook of Industrial Mixing 391-477. Edited by E. Paul, V. Atiemo-Obeng and S. Kresta. New Jersey: John Wiley and sons. ISBN0-471-2619-0

Frisch, U. (1995). Turbulence. UK; Cambridge University Press. ISBN 0 52145 103 5

Goloub, T. and Pugh, R.J. (2003) The role of surfactant head group in the emulsification process: single surfactant systems. *Journal of Colloid and Interface Science* **257** 37-343

Hemrajani, R.R., and Tatterson, G.B. (2004) Mechanically stirred vessels. In Handbook of Industrial Mixing 34-391. Edited by E.Paul, V.Atiemo-Oeng and S. Kresta. New Jersey: John wiley and Sons. ISBN 0 471 26919 0

Hinze(1955). Fundamentals of the Hydrodnamic Mechanism of Splitting in Dispersion Processes. *A.I.Ch.E Journal* **1** 3 289-295

Holland, F.A. and Bragg, R. (1995) Fluid Flow for Chemical Engineers. 2nd Edition. Great Britain; Edward Arnold, a division of Hodder Headline plc. ISBN 0 34061058 1

Jahoda, M., Machon, V. (1994) Homogenisation of liquids in tanks stirred by multiple impellers. *Chem. Eng. Technol*. **17** 95-101

Kolmogorov, A.N. (1941a). The local structure of turbulence in incompressible viscous fluid for very large Reynolds numbers. *Dokl. Akad. Nauk SSSR* **30** 4. Translated and republished in *Proc. R. Soc. Lond. A*. (1991) **434**, 9-13

Kolmogorov, A.N. (1941c). Dissipation of energy in the locally isotropic turbulence. Dokl. Akad. Nauk SSSR 32 1. Translated and republished in Proc. R. Soc. Lond. A. (1991) 434, 15-17

Konno, M., Aoki, M. and Saito, S. (1983) Scale effect on breakup process in liquid-;iquid agitated tanks. *Journal of Chem. Eng. of Japan.* **16** 4 312-319

Koshy, A., Das, T.R. and Kumar, R. (1988) Effects of surfactants on drop breakage in turbulent liquid dispersions. *Chem. Eng. Sci.* **43** 3 649-654

Kowalski, A.J., Watson, S. and Wall, K. Dispersion of nanoparticle clusters by ball milling. *Journal of Dispersion Science and Technology* **29** 4 600-6004

Kresta, S.M., Krebs, R., and Martin, T.(2004). The future of mixing research. *Chem. Eng. Technol*. **27** 3 208-214

Mlynek, Y. and Resnick, W. (1972). Drop sizes in an agitated liquid-liquid system. *A.I.Ch.E. Journal* **18** 1 122-127

Narsimhan, G., Gupta, J.P. and Ramkrishna, D. (1979) A model for transitional breakage probability of droplets in agitated lean liquid-liquid dispersions. *Chem. Eng. Sci.* **34** 57-265

Narsimhan, G., Nejfelt, G, and Ramkrishna, D. (1984) Breakage functions for droplets in agitated liquid-liquid dispersions. *A.I.Ch.E. Journal* **30** 3 457-467

Pacek, A.W., Man, C.C. and Nienow, A.W. (1988) On the Sauter mean diameter and size distributions inturbulent liquid/liquid dispersions in a stirred vessel. Chem. Eng. Sci. 53 11 2005-2011

Ramkrishna, D. (1974) Drop-breakage in Agitated liquid-liquid dispersions. *Chem. Eng. Sci.* **29** 989-992

Ramkrishna, D. (2000) Population Balances. San Diego. Academic Press. ISBN 0-12-576970-9

Ranade, V.V., Bourne, J.R. and Joshi, J.B. (1991) Fluid Mechanics and Blending in agitated tanks. *Chem. Eng. Sci*. **46** 8 1883-1893

Ruiz, M.C. and Padilla, R. (2004) Analysis of breakage functions for liquid-liquid dispersions. Hydrometallurgy 72 245-258

Ruiz, M.C.,Lermanda, P. Padilla, R. (2002) Drop size distribution in a batch mixer under breakage conditions. *Hydrometallurgy* **63** 65-74

Ryan, C. and Thapar, N. (2008) Experience still plays a crucial role for rotor/stator devices. Retrieved 15/08/09 from www.chemicalprocessing.com/articles/2008/049.html

Sathyagal, A.N., Ramkrishna, D, and Narsimhan, G. (1996) Droplet breakup in stirred dispersion. Breakage functions from experimental drop size distributions. *Chem. Eng. Sci*. **51** 9 1377-1391

Shelley, S. (2004) Taking high shear mixing to the next level. *Chemical Engineering* April 2004 24-26

Sleicher (1962) Maximum stable drop size in turbulent flow. *A.I.Ch.E. Journal* **8** 4 471-477

Stamatoudis, M. and Tavlarides,L.L. (1981) The effect of impeller rotational speed on the drop size distributions of viscous liquid-liquid dispersions in agitated vessels. *The Chemical Engineering Journal* **21** 77-78

Taylor (1934). The formation of emulsions in definable fields of flow. *Proc. R. Soc. Lond. A* **146**, 501-523

Taylor, G. (1953a) Dispersion of soluble matter in solvent flowing slowly through a tube. *Proc. Roy. Soc. A* **219** 18-203

Taylor, G. (1954) The dispersion of matter in turbulent flow through a pipe. Proc. R. Soc. Lond. A 446-468

Utomo, A., Baker, M., Pacek, A.W. (2009) The effect of rotor stator geometry on the flow patern and energy dissipation rate in a rotor-stator mixer. *Chemical Engineering Research and Design* **87**, 533-542

Wang, C.Y. and Calabrese, R.V. (1986) Drop breakup in turbulentstirred tank contactors. Part II Relative influence of viscosity and interfacial tension. *A.I.Ch.E. Journal* **32** 4 667-676